International Journal of Solids and Structures 51 (2014) 1075–1088

Contents lists available at ScienceDirect

International Journal of Solids and Structures

journal homepage: www.elsevier.com/locate/ijsolstr

Statistical model of nearly complete elastic rough surface contact

Y. Xu, R.L. Jackson *, D.B. Marghitu

Department of Mechanical Engineering, Auburn University, Auburn, AL 36849, United States

ARTICLE INFO

Article history:
Received 2 August 2013
Received in revised form 14 November 2013
Available online 12 December 2013

Keywords:
Elasticity
Contact mechanics
Fracture mechanics
Roughness
Statistical method

ABSTRACT

In the area of homogeneous, isotropic, linear elastic rough surface normal contact, many classic statistical models have been developed which are only valid in the *early contact* when real area of contact is infinitesimally small, e.g., the Greenwood–Williamson (GW) model. In this article, newly developed statistical models, built under the framework of the (i) GW, (ii) Nayak–Bush and (iii) Greenwood's simplified elliptic models, extend the range of application of the classic statistical models to the case of *nearly complete contact*. Nearly complete contact is the stage when the ratio of the real area of contact to the nominal contact area approaches unity. At nearly complete contact, the non-contact area consists of a finite number of the non-contact regions (over a finite nominal contact area). Each non-contact region is treated as a mode-I "crack". The area of each non-contact region and the corresponding trapped volume within each non-contact region are determined by the analytical solutions in the linear elastic fracture mechanics, respectively. For a certain average contact pressure, not only can the real area of contact be determined by the newly developed statistical models, but also the average interfacial gap. Rough surface is restricted to the geometrically-isotropic surface, i.e., the corresponding statistical parameters are independent of the direction of measurement. Relations between the average contact pressure, non-contact area and average interfacial gap for different combinations of statistical parameters are compared between newly developed statistical models. The relations between non-contact area and average contact pressure predicted by the current models are also compared with that by Persson's theory of contact. The analogies between the classic statistical models and the newly developed models are also explored.

1. Introduction

Elastic rough surface contact models have been developed for more than 50 years since the first one created by Archard (1957). Because of the complexity of the boundary conditions on the contact interfaces, i.e., the surface traction distribution and surface displacement field, the elastic rough surface contact problem cannot be completely solved analytically except for the case when contact becomes complete.[1] The statistical based model is one of the approximate models and was first introduced by Greenwood and Williamson (1966). This is the first model combining the random process with the elastic contact model (Hertzian spherical contact model). Nayak, 1971 modeled the rough surface as a two-dimensional (2D) isotropic, Gaussian, random process, which is referred to as *Nayak's random theory*. Bush and Thomas, 1982 applied Nayak's random theory in the elastic rough surface contact model (Nayak–Bush model) by assuming that the asperities are axisymmetric. Bush et al., 1975 developed, up till now, the most complete statistical model (BGT model) based on Nayak's random theory. Utilization of the Hertzian elliptic contact model complicates the BGT model. Greenwood, 2006 reduced the complexity of the BGT model by introducing an mildly Hertzian elliptic contact model which is only valid for the elliptic asperities with similar principle curvatures. This model is referred to as *Greenwood's simplified elliptic model*. A good agreement can be found between the BGT model and Greenwood's simplified elliptic model (Greenwood, 2006). Those statistical models, discussed above, are now referred to as the *classic* statistical models. One of the main assumptions adopted in the classic statistical models is that the interactions between the neighboring contacting asperities, due to the elasticity of the substrate, are ignored, which limits the application of the classic statistical models within the light load (real area of contact $\ll$ nominal contact area) range.

Nearly all the newly developed statistical models (Bush et al., 1976; O'Callaghan and Cameron, 1976; Francis, 1977; McCool and Gassel, 1981) after the Greenwood and Williamson (GW) model restrict their application within the case of *early contact* where the real area of contact is infinitesimally small. Few attempts have been made to introduce the asperity interaction (equivalently, the elasticity of the substrate) in the classic statistical model (Zhao and Chang, 2001, e.g., Ciavarella et al., 2008). *Nearly complete contact* is defined as the stage where isolated *non-contact regions* (easily visualized as "islands") of infinitesimally small areas are surrounded by the

* Corresponding author. Tel.: +1 334 844 3340.
E-mail addresses: yang.xu@auburn.edu (Y. Xu), robert.jackson@eng.auburn.edu (R.L. Jackson), MARGHDB@auburn.edu (D.B. Marghitu).

[1] Here we implicitly assume that the geometry of the rough surface is *deterministic*.

0020-7683/$ - see front matter © 2013 Elsevier Ltd. All rights reserved.
http://dx.doi.org/10.1016/j.ijsolstr.2013.12.005

Nomenclature

A	real area of contact, i.e., size of domain Ω_c
A^*	contact ratio, $A^* = A/A_n$
A_n	nominal contact area, i.e., the size of Ω
C	rigid body displacement on the plane $z = 0$ of an elastic half-space
$C(r)$	circumference of an ellipse
C_1, C_2	constants, $C_1 = \alpha/(2\alpha - 3)$ and $C_2 = C_1\left(\frac{12}{\alpha}\right)^{1/2}$
E	Young's modulus of equivalent rough surface
$E[\bullet]$	average value of the process inside the square bracket
E^*	effective material modulus, $\frac{1}{E^*} = \frac{1-\nu_1^2}{E_1} + \frac{1-\nu_2^2}{E_2}$
$E_i, i = 1,2$	Young's modulus of rough surface 1 and 2
K_I	stress intensity factor of a mode-I crack
P	total contact load over the domain Ω
P^*	dimensionless contact load at early contact, $P^* = P/(E^* A_n)$
R	average radius of curvature of the asperities
S	power spectrum density of a rough surface
V	variance of the "pressure surface", $p = p_c(x,y)$, $V = \sqrt{m_0^p}$
Ω	nominal contact domain
Ω_c, Ω_{nc}	contact and non-contact domains
Φ	probability density function of the asperity height of a rough surface (or "pressure surface")
α	bandwidth parameter: $\alpha = \frac{m_0 m_4}{m_2^2}$
α_1^p	dimensionless parameter $\alpha_1^p = \frac{m_0^p}{\sqrt{m_2^p}} \frac{1}{E^* \sigma}$
$\overline{A}$	non-contact area, i.e., size of domain Ω_{nc}
$\overline{A}^*$	non-contact ratio, i.e., $\overline{A}^* = 1 - A^*$
$\overline{A}_n$	area of each non-contact region
$\overline{V}_i$	trapped volume within a non-contact region
$\bar{g}$	average interfacial gap
$\bar{g}^*$	dimensionless average interfacial gap, $\bar{g}^* = \bar{g}/\sigma$
$\bar{p}$	average pressure over the domain Ω
$\bar{p}^*$	dimensionless average pressure, $\bar{p}^* = \bar{p}/\sigma_s^p$ in modified GW model and $\bar{p}^* = \bar{p}/\sqrt{m_0^p}$ in modified Nayak–Bush and Greenwood's simplified model
$\bar{p}_c$	critical value of the average pressure across which rough contact becomes complete
$\mathbf{J}$	Jacobian
η	peak density in a random process $[1/m^2]$
κ_1, κ_2	half of the positive maximum and minimum principle "curvatures" of the asperity of the "pressure surface", $p = -p_c(x,y)$ $[Pa/m^2]$
κ_1^*, κ_2^*	dimensionless principle curvatures of the local asperities, $\kappa_i^* = \kappa_i/\sqrt{m_4}, i = 1,2$
κ_m	mean (positive) curvature
$\mathcal{F}$, $\mathcal{F}^{-1}$	Fourier transform and inverse Fourier transform operators
ν	Poisson's ratio of equivalent rough surface
$\nu_i, i = 1,2$	Poisson's ratio of rough surface 1 and 2
σ	root mean square roughness of the surface
σ_s	root meant square of the asperity height
erfc()	complementary error function
erf()	error function
$\widetilde{A}_i$	tensile stress area, i.e., the area of tensile stress in $p_2(x,y)$ within each non-contact region
ξ, ζ	new coordinates, $\xi = x'$, $\zeta = \sqrt{\frac{\kappa_2}{\kappa_1}} y'$
$\xi_i, i = 1,\ldots,6$	random variables in the Nayak's random theory
a_n, b_n	semi-major and semi-minor axes of the elliptic non-contact region, $\overline{A}_n$
d	surface separation between mean levels of two nominally flat rough surface or between mean level of an effective rough surface and a rigid flat
d^*	dimensionless surface separation, $d^* = d/\sigma_s^h$ in original GW model and $d^* = d/\sqrt{m_0^h}$ in original Nayak–Bush and Greenwood's simplified model
e	eccentricity
$g(r)$	crack opening displacement of an axisymmetric mode-I crack
$g(x,y)$	gap distribution between the contact interfaces
h	height of the equivalent rough surface, $h = h_1 + h_2$
$h_i, i = 1,2$	height of rough surface 1 and 2, $E[h_i] = 0$
m	distance between mean level and mean asperity level
$m_i, i = 0,2,4$	spectral moments of an isotropic rough surface
p	normal contact pressure distribution acting on the boundary, $z = 0$, of a half-space
p_1	contact pressure distribution at complete contact (see Eq. (9))
p_2	contact pressure distribution acting only on the non-contact regions (see Eq. (10))
p_c	normal traction distribution at complete contact where $u_z(x,y) = h(x,y)$
q_x, q_y	tangential traction distributions in the x and y directions on the boundary, $z = 0$, of a half-space
r	polar coordinate, $r = \sqrt{\xi^2 + \zeta^2}$
s	semi-sum of the dimensionless principle curvatures of the local asperities: κ_1^* and κ_2^*, i.e., $s = -(\kappa_1^* + \kappa_2^*)$
u	dimensionless (negative) mean curvature, $u = -\kappa_m/\sqrt{m_4}$
$u_i, i = x,y,z$	surface displacement fields due to the given traction distributions on the boundary, $z = 0$, of a half-space
w	amplitude of the frequency vector $\mathbf{w}$
w_x, w_y	frequency components in the x and y directions
x', y'	local coordinates of each non-contact region centered about its centroid (see Fig. 6)
x, y, z	Cartesian coordinates
$\mathbf{E}$	complete elliptic integral of second kind
$\mathbf{w}$	frequency vector contains the frequencies in the x and y directions

Superscript

h	for the rough surface
p	for the "pressure surface"
$*$	dimensionless symbol, except for the effective material modulus, E^*

Abbreviation

GW	Greenwood and Williamson model
BGT	Bush, Gibson and Thomas model

contact area (likewise visualized as the "sea") when the average contact pressure is extremely high. The systematic study of nearly complete contact has received less attention compared to the early contact case even though it has many applications, such as the leakage of static seals, electrical contacts and tire/road interaction.

Johnson et al. (1985) derived the asymptotic solutions of the rough contact problem of an elastic half-space with slightly (bi-) sinusoidal waviness in contact with a rigid flat at nearly complete contact. They treated the gaps between the deformed waviness and the rigid flat as mode-I "cracks". Based on the concept of the *stress intensity factor* (SIF) in fracture mechanics, they obtained the approximate analytic solution to the relation between the average contact pressure and non-contact area within a complete period.

Manners and Greenwood (2006) explored the possibility of obtaining an asymptotic solution at nearly complete rough surface contact. They assumed that each "crack" formed between the rough surface and the rigid flat can be closed by introducing a parabolic tensile stress distribution acting on its surface. Eliminating this tensile stress distribution may form a non-contact region which can be determined by setting the corresponding SIF to zero.

Salganik et al. (2009) reported their previous works on the nearly complete rough surface contact. They treated the gaps between the contact interfaces as sockets. They derived the non-contact area and the pressure distribution at the edge of the contact area as a function of the average pressure acting remotely. In their work, they mentioned the idea of building the solution under the framework of the GW model, however according to the cited articles, their model only includes one socket, i.e., only one non-contact region over the entire nominal contact area, which is unrealistic.

The above three articles form the basis of the current study. The pressure distribution at the almost complete contact will be approximated by the method used by Johnson et al. (1985). The size of each non-contact region will be calculated based on the method reported by Manners and Greenwood (2006). Three new statistical models, which is referred to as the *modified statistical models*, are developed under the frameworks of the classic statistical models, namely, the GW, Nayak–Bush and Greenwood's simplified elliptic models. Final forms of the non-contact area and the average interfacial gap, which will be discussed later, are derived in terms of the average contact pressure.

Persson (2002) developed an original model for the elastic, isotropic, Gaussian surface contact. This model together with all the models based on it are referred to as *Persson's theory of contact*. Persson's theory of contact (Persson, 2002; Manners and Greenwood, 2006) gives a strikingly simple relation between the average pressure and real area of contact between a nominally flat rough surface and a rigid flat throughout the whole range from the first touch to the complete contact. Persson (2007) also extended his original contact theory in order to predict the average interfacial separation which is the distance between the mean level of a deformed rough surface and a rigid flat. In the end of the current study, Persson's theory of contact is compared with the newly developed statistical models.

2. Statement of problem

Fig. 1(a) schematically shows the *frictionless, non-adhesive, dry* contact occurring between two homogeneous, isotropic, linear elastic half-spaces with nominally flat rough surfaces on the boundaries ($z=0$ planes). Note that the effect of gas or liquid sealed between the contact interfaces is neglected. $h_1(x,y)$ and $h_2(x,y)$ are the heights of rough surfaces of two contact bodies over the entire $z=0$ planes. Two rough interfaces are assumed to be smooth only within a certain range of wavelengths, since, in practice, the rough surfaces data are measured from the surfaces of finite sizes with limited resolutions. The upper limit is the dimension of the nominal contact area and the lower limit twice the resolution. The Young's modulus and Poisson's ratio of two contact bodies are E_i and v_i, $i=1,2$, respectively. Surface separation between the mean levels of the two nominally undeformed rough surfaces, $h_1(x,y)$ and $h_2(x,y)$, is d.

The above elastic contact problem is equivalent to the one between a rigid flat and an elastic half-space, see Fig. 1(b), with an equivalent rough surface, $h(x,y)=h_1(x,y)+h_2(x,y)$, Young's modulus, E, and Poisson's ratio, v, so that

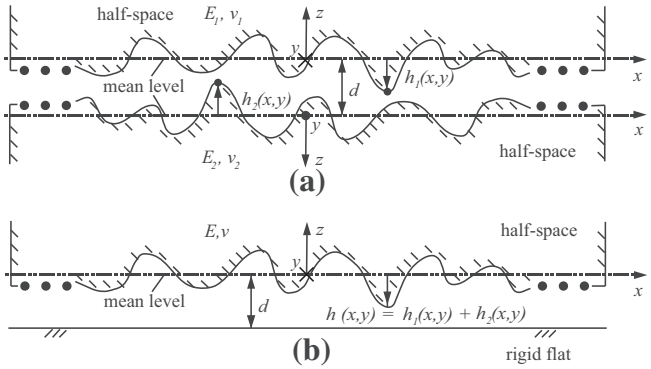

Fig. 1. Elastic contact between (a) two half-spaces with rough surfaces, $h_1(x,y)$ and $h_2(x,y)$, on $z=0$ plane; (b) one half-space with the equivalent rough surface $h(x,y)=h_1(x,y)+h_2(x,y)$ on $z=0$ plane and a rigid flat.

$$\frac{1-v^2}{E}=\frac{1-v_1^2}{E_1}+\frac{1-v_2^2}{E_2}, \tag{1}$$

where $E^*=E/(1-v^2)$ is referred to as the *effective material modulus*. A rigorous proof of the above equivalence can be found in the work of Barber (2003).

Let us define the entire $z=0$ plane of the equivalent rough surface as domain Ω. Since the height of the equivalent rough surface, $h(x,y)=h_1(x,y)+h_2(x,y)$, is absolutely negligible compared with the dimensions of the domain Ω (infinite), the equivalent rough contact body in Fig. 1(b) can be approximated by an elastic half-space.[2] Then the above rough contact problem is transformed into a classic problem of an elastic half-space occupying $z\geqslant 0$. The normal contact pressure, $p(x,y)$, and tangential traction, $q_x(x,y)$ and $q_y(x,y)$, distributions on the domain Ω, give rise to the surface displacement fields, u_i, $i=x,y,z$. The normal contact pressure, $p(x,y)$, and the corresponding surface displacement, $u_z(x,y)$, must satisfy the following inequalities:

$$\begin{aligned} &p(x,y)>0, u_z(x,y)=h(x,y)-d, \quad (x,y)\in\Omega_c,\\ &p(x,y)=0, g(x,y)>0, \quad (x,y)\in\Omega_{nc}, \end{aligned} \tag{2}$$

where Ω_c and Ω_{nc} are the contact and non-contact domains, respectively. $g(x,y)$ is the gap between the contact interfaces. Due to the frictionless assumption, in-plane traction is zero, i.e., $q_x(x,y)=q_y(x,y)=0$. Since the normal displacement, $u_z(x,y)$, is dominant, the in-plane displacement fields, $u_x(x,y)$ and $u_y(x,y)$, are ignored.

Before we move to the next section, one important point needs to be mentioned here. Since the domain Ω is infinite, the real area of contact, A, and contact load, P, are infinite too. The finite contact ratio, A^*, and the average contact pressure, $\bar{p}$, i.e.,

$$A^*=\lim_{A_n\to\infty} A/A_n \text{ and } \bar{p}=\lim_{A_n\to\infty}\frac{1}{A_n}\int_{A_n} p(x,y)\,dA, \tag{3}$$

are more reasonable to describe the infinite rough surface contact. A_n is the nominal contact area which is the size of domain Ω.

3. Contact pressure distribution at nearly complete contact

The above 3-dimensional (3D) elastic *mixed boundary-value problem* can only be solved analytically for several limited cases, e.g., the Hertzian contact of parabolic surfaces. Currently, the rough

[2] The additional requirement for the half-space approximation is that the *mean square slope* of the roughness is much less than one. The half-space approximation is adopted in the majority of the numerical deterministic models (Stanley and Kato, 1997; Polonsky and Keer, 2000; Liu et al., 1999), even though it is not always declared explicitly.

surface contact problems are mainly solved deterministically by the numerical models using various iterative methods (Stanley and Kato, 1997; Polonsky and Keer, 2000; Liu et al., 1999).

Let $E[\bullet]$ be the symbol of taking the average value. In the current study, the rough surface is measured from its mean level, i.e., $E[h] = 0$. When the rough surface comes into complete contact with the rigid flat, the corresponding surface deformation is

$$u_z(x,y) = h(x,y) + C, \tag{4}$$

where the constant term, C, denotes the uniform (rigid body) displacement of the boundary of the half-space. The corresponding contact pressure distribution, $p(x,y)$, between the interfaces is

$$p(x,y) = p_c(x,y) + \bar{p}, \tag{5}$$

where $E[p_c] = 0$. It is very obvious that terms in $p(x,y)$, namely, $p_c(x,y)$ and $\bar{p}$, give rise to the corresponding surface deformation fields, $h(x,y)$ and C, respectively. A schematic representation of the pressure distribution, $p_c(x,y)$, is illustrated in Fig. 2 at the stage of complete contact. In order to achieve the non-adhesive (non-negative pressure) contact, the value of $\bar{p}$ needs to satisfy the following inequality

$$\bar{p} \geqslant |\min(p_c)|. \tag{6}$$

There is a critical value $\bar{p}_c = |\min(p_c)|$ of $\bar{p}$ above which the contact becomes complete. Details of the derivation of $p_c(x,y)$ can be found in Appendix A.

Fig. 3 illustrates the contact domain, Ω_c, and non-contact domain, Ω_{nc}, at nearly complete contact, i.e., $\bar{p}_c - \bar{p} \to 0^+$. At this point, the non-contact domain, Ω_{nc}, consists of infinite sparsely distributed small non-contact regions of size $\bar{A}_i$. Thus, the non-contact ratio, $\bar{A}^* = 1 - A^*$, is

$$\bar{A}^* = \lim_{A_n \to \infty} \frac{1}{A_n} \sum_{i=1}^{\infty} \bar{A}_i. \tag{7}$$

At nearly complete contact, the corresponding pressure distribution, $p(x,y)$, may be approximated by Eq. (5). The accuracy of this equation depends on $\bar{p}_c - \bar{p}$. As $\bar{p}_c - \bar{p}$ increases, the error brought by Eq. (5) may be amplified. However, if we restrict our analysis within a reasonable range of $\bar{p}_c - \bar{p}$, the pressure distribution predicted by Eq. (5) may not deviate much from the real solution. In the non-contact domain, Ω_{nc}, the contact pressure, $p(x,y)$, is zero. Consequently, a truncated form of Eq. (5) may be used to approximate the corresponding pressure distribution for the nearly complete contact case:

$$p(x,y) = \begin{cases} p_c(x,y) + \bar{p} & (x,y) \in \Omega_c, \\ 0 & (x,y) \in \Omega_{nc}, \end{cases} \tag{8}$$

where $\bar{p} < \bar{p}_c$. This truncation method has already been used by Johnson et al. (1985) in approximating the contact pressure between a slightly (bi-) sinusoidal waviness and a rigid flat at nearly complete contact case.

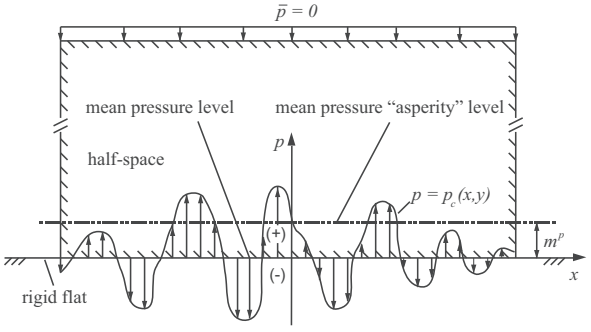

Fig. 2. The cross-section of a part of the normal traction distribution, $p_c(x,y)$, due to a given surface displacement $u_z(x,y) = h(x,y)$ on the domain Ω.

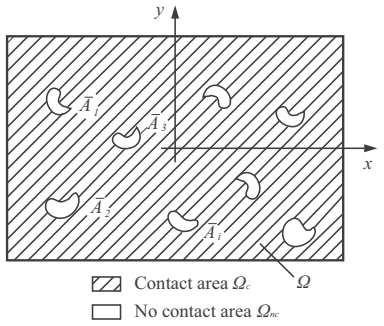

Fig. 3. Part of domain Ω consists of the contact domain, Ω_c, and the non-contact domain, Ω_{nc}, at nearly complete contact.

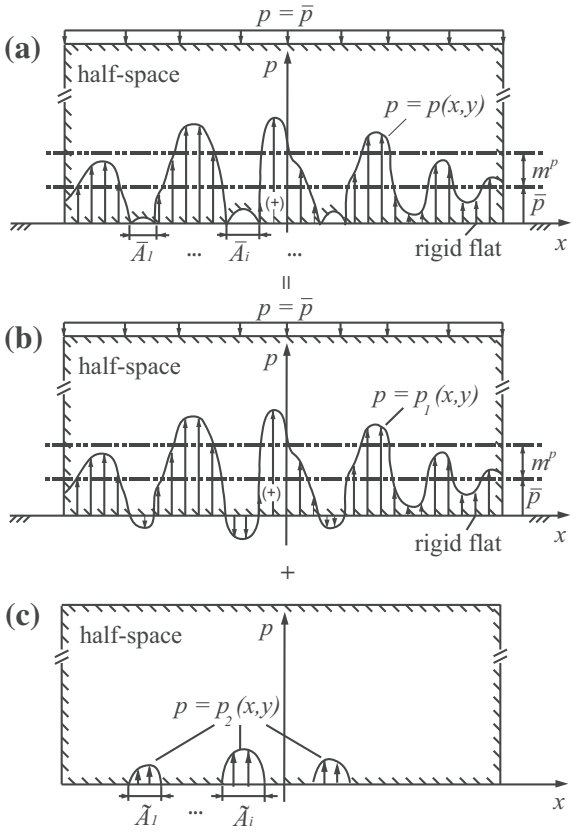

Fig. 4. Schematic representations of the decomposition of (a) a nearly complete contact with pressure distribution $p(x,y)$ into (b) a complete contact with $p_1(x,y)$ and (c) a pressurized half-space with $p_2(x,y)$ only acting on the non-contact domain Ω_{nc}.

Fig. 4(a) shows the cross-section of a part of the contact pressure distribution, $p(x,y)$, and the corresponding deformed profile of the rough surface. According to Eqs. (5) and (8), $p(x,y)$ for the nearly complete contact is obtained by the superposition of $p_1(x,y)$ as shown in Fig. 4(a) and $p_2(x,y)$ as shown in Fig. 4(c):

$$p_1(x,y) = p_c(x,y) + \bar{p} \quad (x,y) \in \Omega, \tag{9}$$

and

$$p_2(x,y) = \begin{cases} 0 & (x,y) \in \Omega_c, \\ -[p_c(x,y) + \bar{p}] & (x,y) \in \Omega_{nc}, \end{cases} \tag{10}$$

Assuming that the negative pressure in $p_1(x,y)$ is negligible comparing to the positive part (this is true at nearly complete contact), then the average pressure in Fig. 4(a) and (b) can be treated as the same (see the average pressure distributions on the far ends in Fig. 4(a) and (b)).

Since the geometry of the rough surface, $h(x,y)$, and the corresponding pressure distribution, $p_c(x,y)$, at complete contact are very similar, the terminologies, such as asperity and valley, can also be applied to describe the corresponding geometrical feature of $p_c(x,y)$. Here we refer to the geometry of the pressure distribution as the "*pressure surface*".

When $\bar{p}_c - \bar{p} \to 0^+$, the positive pressure distribution, $p_2(x,y)$, in Fig. 4(c) is equivalent to a group of valleys of the "pressure surface" $p_1(x,y)$ below the $p=0$ level in Fig. 5(a). Additionally, $p_2(x,y)$ is also equivalent to a group of asperities of the "pressure surface" $p=-p_c(x,y)$ above the $p=\bar{p}$ level in Fig. 5(b). $\widetilde{A}_i$ in Fig. 4(c) represents each bearing area of the pressure distribution $p_2(x,y)$ on the $p=0$ level. Equivalently, we can also find $\widetilde{A}_i$ in Fig. 5(b) on the level $p=\bar{p}$. $\widetilde{A}_i$ is referred to as the "*tensile pressure area*" in the current study.

Usually the asperities of the rough surface are approximated by the parabolic form (i.e., Hertz contact) in the classic statistical models, e.g., the GW (Greenwood and Williamson, 1966), Nayak–Bush (Bush and Thomas, 1982) and BGT (Bush et al., 1975) models. Similarly, the geometry of $p_2(x,y)$ within each non-contact region can also be described by the parabolic form:

$$p_2(x',y') = (p-\bar{p}) - \kappa_1 x'^2 - \kappa_2 y'^2 \quad (x',y') \in \overline{A}_i, \tag{11}$$

where x' and y' are the local coordinates in each non-contact region. p is the height of the local asperity of the "pressure surface" $p=-p_c(x,y)$ in Fig. 5(b). κ_1 and κ_2 are positive *maximum* and *minimum* semi-principle curvatures of the "pressure surface" $p=-p_c(x,y)$ along the *principle axes* x' and y' which are illustrated for a typical non-contact region in Fig. 6. Note that the dimensions of κ_1 and κ_2 are $[Pa/m^2]$. It is obvious that the shape of the non-contact region is elliptic ($\kappa_1 > \kappa_2$) or circular ($\kappa_1 = \kappa_2$) from the above parabolic form of pressure distribution and is also reasonable to be applied to approximate the shapes of the real non-contact regions at nearly complete contact.

Fig. 6 illustrates a typical elliptic contact region of semi-axes a_i and b_i ($a_i \geqslant b_i$), respectively. Using the following coordinate transformations

$$\xi = x', \quad \zeta = \sqrt{\frac{\kappa_2}{\kappa_1}}y',$$

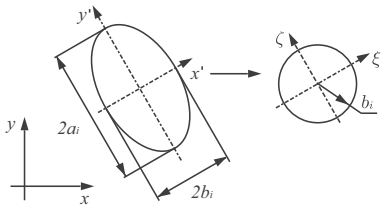

Fig. 6. Schematic representations of (i) an elliptic non-contact region of semi-axes a_i and b_i ($a_i \geqslant b_i$) in the local coordinates x' and y'; (ii) a circular non-contact region of radius b_i in the local coordinates ξ and ζ after coordinate transformations.

we can redefine $p_2(x',y')$ in polar coordinates as follows

$$p_2(r) = (p-\bar{p}) - \kappa_1 r^2, \quad |r| \leqslant b_i, \tag{12}$$

where $r = \sqrt{\xi^2 + \zeta^2}$.

According to the above discussion, we may draw the following conclusion: *Non-contact regions occur at the same locations as those asperities of the "pressure surface", $p=-p_c(x,y)$, which are above the level $p=\bar{p}$.* Consequently, the distribution of the non-contact regions is naturally related with that of the asperities of the "pressure surface", $p=-p_c(x,y)$. *In the rest of this article, the terminology, "pressure surface", is reserved only for describing the geometry of the pressure distribution, $p=-p_c(x,y)$.* In the following two sections, analytical methods in fracture mechanics are applied to determine the area of each non-contact region and the corresponding trapped volume.

4. Area of the "cracks"

One of the assumptions adopted in the classic statistical models, e.g., the GW (Greenwood and Williamson, 1966), Nayak–Bush (Bush and Thomas, 1982) and BGT models (Bush et al., 1975), is that the interaction between neighboring contacting asperities is negligible. This is the main reason that the classic statistical models are only valid in the early contact. Similarly, this assumption can be applied in the current study with a different statement: the interaction between neighboring non-contact regions is negligible. This assumption is reasonable because the pressurized non-contact regions of negligibly small sizes are distributed remotely at the case of nearly complete contact, see Fig. 4(c). Consequently, each non-contact region can be studied individually and one of which is illustrated in Fig. 7(a). The pressure distribution, $p(r)$, can be described in polar coordinates at the vicinity of each

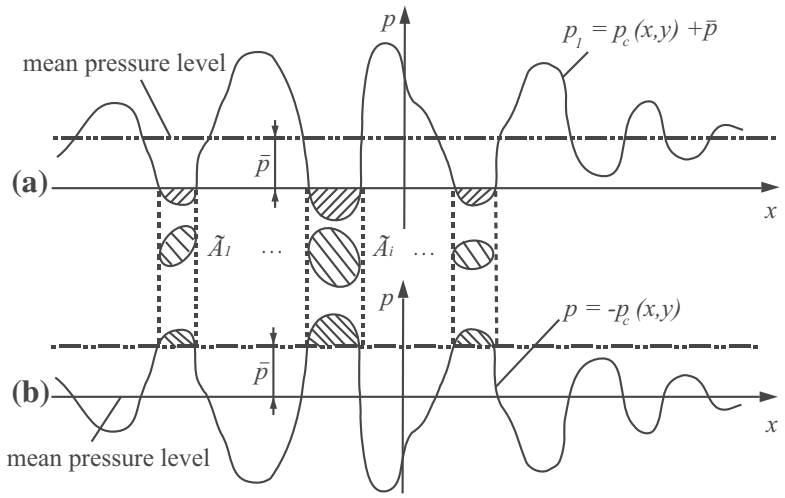

Fig. 5. Schematic representations of (a) the valleys (shaded parts) of the "pressure surface" $p_1(x,y) = p_c(x,y) + \bar{p}$ and (b) the asperities (shaded parts) of the "pressure surface" $p(x,y) = -p_c(x,y)$.

non-contact region due to the axisymmetric form of Eq. (12). According to the previously described decomposition of $p(r)$, Fig. 7(a) can be treated in the same way as the superposition of Fig. 7(b) and (c).

Fig. 7(a) shows the details of the contact between a nominally flat rough surface and a rigid flat at nearly complete contact at the vicinity of a non-contact region which can be treated as a mode-I "crack". Fig. 7(b) shows an uncracked body where the gap is closed due to the negative (tensile) pressure distribution acting on the "crack" surface. Fig. 7(c) shows a cracked body with the pressure distribution, $p_2(r)$ of Eq. (12), acting only on the "crack" surface.

According to Buckner's principle (Buckner, 1958), the stress intensity factors (SIF), K_I, at the edges (A and B) of the "crack", in Fig. 7(a) and (c) are the same. However, it is obvious that no stress singularity exists at those edges since the contact pressure there are zero. As a matter of fact, SIF is zero: $K_I = 0$.

The SIF for the case shown in Fig. 7(c) can be calculated by the following Green's function developed by Barenblatt (1962)

$$K_I = \frac{2}{\sqrt{\pi b_i}} \int_0^{b_i} \frac{rp(r)}{\sqrt{b_i^2 - r^2}} dr = \frac{2b_i}{\sqrt{\pi b_i}} \left[(p - \bar{p}) - \frac{2}{3}\kappa_1 b_i^2 \right], \tag{13}$$

where $p_2(r)$ is replaced by Eq. (12) and b_i is the radius of the non-contact region, $\overline{A}_i$, defined in coordinates (ξ, ζ), see Fig. 6. Setting $K_I = 0$ in Eq. (13), we have the semi-minor axis of the elliptic non-contact region defined in coordinates (x', y')

$$b_i = \sqrt{\frac{3(p - \bar{p})}{2\kappa_1}}, \tag{14}$$

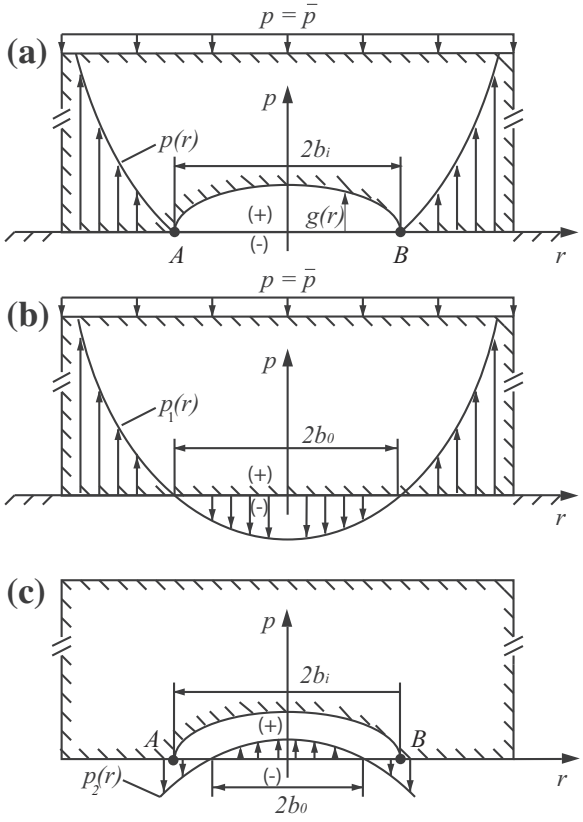

Fig. 7. Schematic representations of (a) contact pressure distribution, $p(r)$, and deformed rough surface at the vicinity of a non-contact region, $\overline{A}_i$; (b) contact pressure distribution, $p_1(r)$, when the gap is closed; (c) contact pressure distribution, $p_2(r)$, acting only on the non-contact region, $\overline{A}_i$.

which is derived by Manners and Greenwood (2006). According to the relation $\zeta = \sqrt{\frac{\kappa_2}{\kappa_1}} y'$, we can also have the semi-major axis of the elliptic non-contact region

$$a_i = \sqrt{\frac{3(p - \bar{p})}{2\kappa_2}}. \tag{15}$$

Johnson et al. (1985) derived the expression of b_i in another way. Firstly, they obtained the crack opening displacement, $g(r)$, shown in Fig. 7(a), based on *Sneddon's solution* (Sneddon, 1946). Since there's no singularity at the edges of the contact region, the derivative $dg(r)/dr = 0$ when $r = b_i$. Derivation of b_i can be found in Appendix B and the expression of b_i is exactly the same as Eq. (14).

Now, the area of the elliptic non-contact region is

$$\overline{A}_i = \pi a_i b_i = \frac{3}{2}\pi \frac{p - \bar{p}}{\sqrt{\kappa_1 \kappa_2}}. \tag{16}$$

For a special case when an asperity of the "pressure surface" is axisymmetric, i.e., $\kappa = \kappa_1 = \kappa_2$, the area of non-contact region is

$$\overline{A}_i = \frac{3}{2}\pi \frac{p - \bar{p}}{\kappa}. \tag{17}$$

According to the statistical contact theory, the contact ratio, $A^*(\bar{p})$, may then be calculated using the following integral:

$$1 - A^*(\bar{p}) = \eta^p \iiint \overline{A}_i(p, \kappa_1, \kappa_2) \Phi^p(p, \kappa_1, \kappa_2) d\kappa_1 d\kappa_2 dp, \tag{18}$$

where η^p is the asperity density of the "pressure surface" and Φ^p is the probability density function (PDF) of the asperity heights of the "pressure surface".

Setting $p_2(r)$ in Eq. (12) to zero, we can obtain the semi-axes a_0 and b_0 of the "tensile stress area" $\widetilde{A}_i$: $b_0 = \sqrt{\frac{p-\bar{p}}{\kappa_1}}$ and $a_0 = \sqrt{\frac{p-\bar{p}}{\kappa_2}}$ and the relation between $\widetilde{A}_i$ and $\overline{A}_i$ is

$$\overline{A}_i = \frac{3}{2}\widetilde{A}_i. \tag{19}$$

Note that $\overline{A}_i$ is larger than the corresponding tensile pressure area. Theoretically, $\overline{A}_i$ should be equal to $\widetilde{A}_i$ in order to guarantee that the contact pressures, $p(r)$, at the contact edges, e.g., A and B in Fig. 7, are zero. However, since $\overline{A}_i > \widetilde{A}_i$, $p(r)$ must have a sudden jump from zero (non-contact region) to positive (contact region) values at edges A and B after the superposition of $p_1(r)$ and $p_2(r)$, which is against the zero boundary condition. This paradox can be explained by the fact that the form of the tensile pressure distribution, $p_2(r)$, is over-simplified as parabolic.

5. Trapped volume in a single "crack"

Based on the crack opening displacement, $g(r)$, derived in Eq. (B.1) in the Appendix B, the trapped volume, $\overline{V}_i$, between each "crack" surface and the rigid flat is

$$\overline{V}_i = \int_0^{b_i} g(r) C(r) dr. \tag{20}$$

Note that the "crack" opening displacement, $g(r)$, is defined in polar coordinates. $C(r)$ is the circumference of the boundary on which "crack" opening displacements share the same value of $g(r)$. In polar coordinates, this boundary is a circle of radius r. Transforming back to the coordinates x' and y', this boundary becomes elliptic with the semi-axes: $r\sqrt{\frac{\kappa_1}{\kappa_2}}$ (major) and r (minor), and $C(r)$ may be written as

$$C(r) = 4r\sqrt{\frac{\kappa_1}{\kappa_2}} \mathbf{E}(e). \tag{21}$$

Now note that $\mathbf{E}(e)$ is the complete elliptic integral of the second kind

$$\mathbf{E}(e) = \int_0^{\pi/2} \sqrt{1 - e^2 \sin^2(\theta)}\, d\theta, \tag{22}$$

and e is the eccentricity of an elliptic crack defined as

$$e = \sqrt{\frac{a_i^2 - b_i^2}{a_i^2}} = \sqrt{1 - \kappa_2/\kappa_1}. \tag{23}$$

Consequently, substituting Eqs. (14), (21), (23) and (B.1) into Eq. (20), the following expression of $\overline{V}_i$ is obtained

$$\overline{V}_i = \frac{16\sqrt{3}}{5\sqrt{2}\pi E^*} \frac{(p - \bar{p})^{5/2}}{\kappa_1 \sqrt{\kappa_2}} \mathbf{E}(e). \tag{24}$$

For the case when the asperities of the "pressure distribution" are axisymmetric, i.e., $\kappa = \kappa_1 = \kappa_2, e = 0, \mathbf{E}(0) = \pi/2$, the expression of $\overline{V}_i$ is simplified to

$$\overline{V}_i = \frac{8\sqrt{3}}{5\sqrt{2}E^*} \frac{(p - \bar{p})^{5/2}}{\kappa^{3/2}}. \tag{25}$$

Finally, the average interfacial gap, $\bar{g}$, can be determined according to the statistical contact theory as

$$\bar{g}^*(\bar{p}) = \eta^p/\sigma \iiint \overline{V}_i(p, \kappa_1, \kappa_2) \Phi^p(p, \kappa_1, \kappa_2) d\kappa_1 d\kappa_2 dp, \tag{26}$$

and $\bar{g}^*$ is the dimensionless form of $\bar{g}$ normalized by the root mean square (r.m.s) roughness σ.

6. Statistics of "pressure surface"

It is widely accepted that a rough surface, $h(x,y)$, is a random process, i.e., it does not have a deterministic form. Since the corresponding "pressure surface" can be determined through the Fourier transform of $h(x,y)$ (see Appendix A), we can expect that the "pressure surface" is also a random process. Consequently, the geometry of the "pressure surface" needs to be described statistically. In order to distinguish the statistics of the "pressure surface" from that of the rough surface, two superscripts "p" and "h" are defined to denote the statistic parameters for the "pressure surface" and rough surface, respectively.

In the following sections, the discussion of the statistics of the "pressure surface" is limited to the case where the corresponding rough surface, $h(x,y)$, is a *random, isotropic, Gaussian* surface. Then, the joint PDF of the rough surface has the following form according to Nayak's random theory (Nayak, 1971)

$$\Phi^h = \Phi^h(\xi_1^h, \xi_2^h, \ldots, \xi_6^h), \tag{27}$$

which is in the function of 6 random variables, $\xi_i^h, i = 1, \ldots, 6$, where

$$\xi_1^h = h, \quad \xi_2^h = \frac{\partial h}{\partial x}, \quad \xi_3^h = \frac{\partial h}{\partial y},$$
$$\xi_4^h = \frac{\partial^2 h}{\partial x^2}, \quad \xi_5^h = \frac{\partial^2 h}{\partial x \partial y}, \quad \xi_6^h = \frac{\partial^2 h}{\partial y^2}, \tag{28}$$

where Φ^h denotes the probability of a rough surface point having a certain combination of height, slopes and curvatures defined by Eq. (28). The complete expression of Φ^h can be found in the work of (Eq. (35) in Nayak (1971)).

For an isotropic surface, these random variables are related to the spectral moments by

$$m_0^h = E[(\xi_1^h)^2], \; m_2^h = E[(\xi_2^h)^2] = E[(\xi_3^h)^2], \; m_4^h = E[(\xi_4^h)^2] = E[(\xi_6^h)^2]. \tag{29}$$

Two problems need to be answered before we apply Nayak's random theory to describe the statistics of the "pressure surface":

1. Under what condition is the "pressure surface" isotropic?
   Isotropy of a surface means the identical statistics along any directions. In a frequency domain, isotropy is represented by the fact that the *power spectrum density* (PSD) of a surface, $S(\mathbf{w}) = S(w)$, is only depend on the amplitude, $w = \sqrt{w_x^2 + w_y^2}$, of the frequency vector $\mathbf{w} = [w_x, w_y]$. From Eq. (A.1), we can obtain the following relation,
   $$p(\mathbf{w}) = \frac{1}{2} E^* \sqrt{w_x^2 + w_y^2} h(\mathbf{w}), \tag{30}$$
   which is the transfer function between the spectrums of the rough surface, $-h(x,y)$, and the corresponding "pressure surface", $-p_c(x,y)$. Taking square of the above transfer function, we can have the relation between the power spectrum density of the rough surface and the "pressure surface",
   $$S[-p_c](\mathbf{w}) = \frac{1}{4}(E^*)^2 w^2 S[-h](\mathbf{w}). \tag{31}$$
   Thus, the "pressure surface" is isotropic as long as the rough surface is isotropic.
2. Under what condition is the "pressure surface" Gaussian?
   Manners and Greenwood (2006) pointed out that "A key feature of the Gaussian profile is that it can be regarded as being the sum of an infinite number of infinitesimally small, uncorrelated, sinusoidal waves". According to Eq. (A.2) in Appendix A, the "pressure surface" is Gaussian as long as the corresponding rough surface, $h(x,y)$, is Gaussian.
   Thus, by following the expression of the above Φ^h, the joint PDF of the "pressure surface" can be written as
   $$\Phi^p = \Phi^p(\xi_1^p, \xi_2^p, \ldots, \xi_6^p), \tag{32}$$
   where
   $$\xi_1^p = p, \quad \xi_2^p = \frac{\partial p}{\partial x}, \quad \xi_3^p = \frac{\partial p}{\partial y},$$
   $$\xi_4^p = \frac{\partial^2 p}{\partial x^2}, \quad \xi_5^p = \frac{\partial^2 p}{\partial x \partial y}, \quad \xi_6^p = \frac{\partial^2 p}{\partial y^2}. \tag{33}$$
   For an isotropic "pressure surface", these random variables are related to the spectral moments by
   $$m_0^p = E[(\xi_1^p)^2], \; m_2^p = E[(\xi_2^p)^2] = E[(\xi_3^p)^2], \; m_4^p = E[(\xi_4^p)^2] = E[(\xi_6^p)^2]. \tag{34}$$
   Note that the dimensions of m_0^p, m_2^p and m_4^p are $\left[Pa^2\right]$, $\left[Pa^2/m^2\right]$ and $\left[Pa^2/m^4\right]$.

7. Application of classic statistical models in the nearly complete contact

In the previous sections, we derive (i) the area, $\overline{A}_i$, of each non-contact region (Eq. (16)); (ii) the trapped volume, $\overline{V}_i$, within each non-contact region (Eq. (24)) and (iii) the statistical framework, i.e., the PDF, Φ^p, and spectral moments, $m_n^p, n = 0, 2, 4$, of the "pressure surface".

According to the expressions of contact ratio, A^*, and average interfacial gap, $\bar{g}^*$, in Eqs. (18) and (26), an appropriate PDF, Φ^p, needs to be found. In the following sections, PDFs used in the GW (Greenwood and Williamson, 1966), Nayak–Bush (Bush and Thomas, 1982) and Greenwood's simplified elliptic (Greenwood, 2006) models are applied to build three newly developed statistical models for the case of nearly complete contact, respectively.

7.1. Modified Greenwood and Williamson (GW) model

In the original GW model, the PDF of the asperity is Gaussian which depends only on one random variable, ξ_1^h, and the effects of the curvatures on the PDF are neglected. Similarly, the PDF of

the asperity of the "pressure surface" can follow the same form of that in the original GW model which can be written as

$$\Phi^p(\xi_1^p) = \frac{1}{\sqrt{2\pi}\sigma_s^p}\exp\left[-\frac{(\xi_1^p - m^p)^2}{2(\sigma_s^p)^2}\right], \tag{35}$$

where σ_s^p is the r.m.s of the asperity heights of the "pressure surface", m^p is the distance between the mean asperity level and mean level of the "pressure surface" (see Fig. 2). In the original GW model, the shape of each asperity is assumed to have a constant radius of curvature, R^h, and thus a constant R^p is used to approximate the average radius of curvature of the asperities of the "pressure surface". Note that h and p on R^h and R^p are superscripts not powers and the dimension of R^p is $[m^2/Pa]$. Substituting $2\kappa = 1/R^p$ into Eqs. (17) and (25), then the non-contact region, $\overline{A}_i$, is

$$\overline{A}_i = 3\pi R^p(\xi_1^p - \bar{p}), \tag{36}$$

and the trapped volume, $\overline{V}_i$, between each "crack" surface and the rigid flat is

$$\overline{V}_i = \frac{16\sqrt{3}}{5E^*}(R^p)^{3/2}(\xi_1^p - \bar{p})^{5/2}. \tag{37}$$

According to Eq. (18), the contact ratio, A^*, is formulated as

$$1 - A^*(\bar{p}) = 3\pi\eta^p R^p\int_{\bar{p}}^{\infty}(\xi_1^p - \bar{p})\Phi^p(\xi_1^p)d\xi_1^p. \tag{38}$$

According to Eq. (26), the average gap, $\bar{g}^*$, is

$$\bar{g}^*(\bar{p}) = \frac{16\sqrt{3}}{5E^*\sigma}\eta^p(R^p)^{3/2}\int_{\bar{p}}^{\infty}(\xi_1^p - \bar{p})^{5/2}\Phi^p(\xi_1^p)d\xi_1^p, \tag{39}$$

The infinite upper limit of the contact pressure stems naturally from the Gaussian "pressure surface" as long as the corresponding rough surface is Gaussian. Additionally, from Eq. (38), we can have the following conclusion that a complete contact cannot be achieved unless the average contact pressure, $\bar{p}$, approaches infinity. This has also been discovered by Ciavarella et al. (2000), Manners (2000), Persson (2002), Manners and Greenwood (2006), Jackson (2011), etc. Recently, an interesting conclusion has been drawn by Kudish et al. (2013) that the complete contact of a *twice continuously differentiable* rough surface may be achieved under a sufficiently large average pressure.

McCool (1987) collected the closed-form expressions of inputs for the GW model derived by Nayak (1971) and Bush et al. (1976). Equivalently they can be applied here to determine η^p, m^p, R^p and σ_s^p

$$\eta^p = \frac{1}{6\sqrt{3}\pi}\left(\frac{m_4^p}{m_2^p}\right),\quad m^p = 4\left(\frac{m_0^p}{\pi\alpha^p}\right)^{1/2},$$
$$R^p = 0.375\left(\frac{\pi}{m_4^p}\right)^{1/2},\quad \sigma_s^p = \left(1 - \frac{0.8968}{\alpha^p}\right)^{1/2}(m_0^p)^{1/2}, \tag{40}$$

where α^p is the bandwidth parameter of the "pressure surface": $\alpha^p = \frac{m_0^p m_4^p}{(m_2^p)^2}$.

The following dimensionless variables are now defined: $\xi_1^{p*} = \xi_1^p/\sigma_s^p$ and $\bar{p}^* = \bar{p}/\sigma_s^p$ as well as a dimensionless form of the Gaussian distribution (Eq. (35))

$$\Phi^{p*}(\xi_1^{p*}) = \sigma_s^p\Phi^p(\xi_1^{p*}) \tag{41}$$

Substituting the above dimensionless variables into Eqs. (38) and (39), we have

$$1 - A^*(\bar{p}^*) = 3\pi\eta^p R^p\sigma_s^p\int_{\bar{p}^*}^{\infty}(\xi_1^{p*} - \bar{p}^*)\Phi^{p*}(\xi_1^{p*})d\xi_1^{p*}, \tag{42}$$

$$\bar{g}^*(\bar{p}^*) = \frac{16\sqrt{3}}{5}\frac{\eta^p(R^p)^{3/2}}{E^*\sigma}(\sigma_s^p)^{5/2}\int_{\bar{p}^*}^{\infty}(\xi_1^{p*} - \bar{p}^*)^{5/2}\Phi^{p*}(\xi_1^{p*})d\xi_1^{p*}. \tag{43}$$

Substituting McCool's input (Eq. (40)) and a new defined dimensionless variable: $\alpha_1^p = \frac{m_0^p}{\sqrt{m_2^p}}\frac{1}{E^*\sigma}$ into the above equations, the contact ratio is

$$1 - A^*(\bar{p}^*) = \frac{\sqrt{3\pi}}{16}\sqrt{\alpha^p - 0.8968}\int_{\bar{p}^*}^{\infty}(\xi_1^{p*} - \bar{p}^*)\Phi^{p*}(\xi_1^{p*})d\xi_1^{p*}, \tag{44}$$

and the average interfacial gap is

$$\bar{g}^*(\bar{p}^*)/\alpha_1^p = \frac{\sqrt{3}}{10\sqrt{2}(\pi)^{1/4}}\frac{(\alpha^p - 0.8968)^{5/4}}{\alpha^p}\int_{\bar{p}^*}^{\infty}(\xi_1^{p*} - \bar{p}^*)^{5/2}\Phi^{p*}(\xi_1^{p*})d\xi_1^{p*}. \tag{45}$$

Note that for a given dimensionless average pressure, $\bar{p}^*$, the corresponding dimensionless non-contact area, $1 - A^*$, and average interfacial gap, $\bar{g}^*/\alpha_1^p$, only depend on α^p. In the following discussed statistical models, $\bar{p}^*$ is all normalized by $\sqrt{m_0^p}$, while here in the modified GW model $\bar{p}^*$ is normalized by σ_s^p. Since $\sigma_s^p = \left(1 - \frac{0.8968}{\alpha^p}\right)^{1/2}(m_0^p)^{1/2}$, the above observation will still hold if $\bar{p}^*$ used in the GW model is normalized by $\sqrt{m_0^p}$ in stead of σ_s^p.

7.2. Modified Nayak–Bush model

Nayak (1971) developed a random theory to describe the statistics of a *random, isotropic, Gaussian* rough surface by introducing the joint PDF, $\Phi^h = \Phi(\xi_1^h, \ldots, \xi_6^h)$. The definitions of $\xi_1^h, \ldots, \xi_6^h$ can be found in Eq. (28). Since the slopes of the peaks of the local asperities are zero,

$$\xi_2^h = \xi_3^h = 0. \tag{46}$$

Nayak defined a (positive) mean curvature, κ_m^h, which is the average of the principle curvatures, $2\kappa_1^h$ and $2\kappa_2^h$, of the local asperity, i.e.,

$$\kappa_m^h = \kappa_1^h + \kappa_2^h. \tag{47}$$

Since the sum of the principle curvatures of the asperity is equal to the sum of the curvatures along any two orthogonal directions, κ_m^h can also be written as

$$\kappa_m^h = -\frac{1}{2}\left(\frac{\partial^2\xi_1^h}{\partial x^2} + \frac{\partial^2\xi_2^h}{\partial y^2}\right) = -\frac{1}{2}(\xi_4^h + \xi_6^h). \tag{48}$$

Embedding the zero slope condition ($\xi_2^h = \xi_3^h = 0$) and the above equation in the expression of Φ^h and after tedious mathematical manipulation, Nayak obtained the PDF of the asperity, $\Phi^h(\xi_1^h, \kappa_m^h)$, in terms of two random variables, ξ_1^h and κ_m^h (see Eq. (61) in Nayak (1971)).

Similarly, if we assume the rough surface is random, isotropic, and Gaussian, we can obtain the PDF of the asperity of the "pressure surface". Following the notation suggested by Greenwood (2006), we have

$$\Phi^{p*}(\xi_1^{p*}, u^p) = \frac{3\sqrt{C_1}}{2\pi}\exp\left[-C_1(\xi_1^{p*})^2\right]\left[3(u^p)^2 - 2 + 2\exp\left(-\frac{3}{2}(u^p)^2\right)\right] \times \exp\left[-\frac{1}{2}\left(3C_1(u^p)^2 + \sqrt{3}C_2u^p\xi_1^{p*}\right)\right], \tag{49}$$

where

$$\xi_1^{p*} = \xi_1^p\Big/\sqrt{m_0^p},\quad u^p = -\kappa_m^p\Big/\sqrt{m_4^p},$$
$$C_1 = \alpha^p\Big/(2\alpha^p - 3),\quad C_2 = C_1\left(\frac{12}{\alpha^p}\right)^{1/2}. \tag{50}$$

ξ_1^{p*} is the dimensionless asperity height of the "pressure surface". κ_m^p is the (positive) mean curvature of the asperity of the "pressure surface", i.e.,

$$\kappa_m^p = -\frac{1}{2}\left(\frac{\partial^2 \xi_1^p}{\partial x^2} + \frac{\partial^2 \xi_1^p}{\partial y^2}\right) = -\frac{1}{2}(\xi_4^p + \xi_6^p), \tag{51}$$

and u^p is a dimensionless (negative) mean curvature. Constants, C_1 and C_2, are only in terms of α^p. It is obvious that $\Phi^{p*}(\xi_1^{p*}, u^p)$ is dimensionless.

Bush and Thomas (1982) applied the PDF of the asperity, $\Phi^h(\xi_1^h, \kappa_m^h)$, derived by Nayak (1971) in the statistical elastic contact model by assuming that the asperities are hemispheres of curvatures κ_m^h. Similarly, by assuming that the asperities of the "pressure surface" are hemispheres and substituting $2\kappa = \kappa_m^p$ into Eqs. (17) and (25), the non-contact region, $\overline{A}_i$, is

$$\overline{A}_i = \frac{3\pi}{\kappa_m^p}(\xi_1^p - \bar{p}), \tag{52}$$

and the trapped volume, $\overline{V}_i$, between the "crack" surface and the rigid flat is

$$\overline{V}_i = \frac{16\sqrt{3}}{5E^*}\frac{(\xi_1^p - \bar{p})^{5/2}}{(\kappa_m^p)^{3/2}}. \tag{53}$$

Replacing the variables, ξ_1^p, $\bar{p}$ and κ_m^p, with the corresponding dimensionless ones, the following forms can be derived

$$\overline{A}_i = 3\pi\left(\frac{m_0^p}{m_4^p}\right)^{1/2}(\xi_1^{p*} - \bar{p}^*)(-u^p)^{-1},$$
$$\overline{V}_i = \frac{16\sqrt{3}}{5E^*}\frac{(m_0^p)^{5/4}}{(m_4^p)^{3/4}}(\xi_1^{p*} - \bar{p}^*)^{5/2}(-u^p)^{-3/2}, \tag{54}$$

where $\bar{p}^* = \bar{p}/\sqrt{m_0^p}$.

According to Eqs. (18) and (26), we may have the contact ratio, $A^*(\bar{p}^*)$, and average interfacial gap, $\bar{g}^*(\bar{p}^*)$, in the following forms

$$1 - A^*(\bar{p}^*) = \frac{\sqrt{\alpha^p}}{2\sqrt{3}}\int_{\bar{p}^*}^{\infty}\int_{-\infty}^{0}(\xi_1^{p*} - \bar{p}^*)(-u^p)^{-1}\Phi^{p*}(\xi_1^{p*}, u^p)du^p d\xi_1^{p*}, \tag{55}$$

and

$$\bar{g}^*(\bar{p}^*)/\alpha_1^p = \frac{8}{15\pi}(\alpha^p)^{1/4}\int_{\bar{p}^*}^{\infty}\int_{-\infty}^{0}(\xi_1^{p*} - \bar{p}^*)^{5/2}(-u^p)^{-3/2}\Phi^{p*}(\xi_1^{p*}, u^p)du^p d\xi_1^{p*}, \tag{56}$$

where $\alpha_1^p = \frac{m_0^p}{\sqrt{m_2^p}}\frac{1}{E^*\sigma}$.

Note the similarity here to that declared in the end of Section 7.1: for a fixed dimensionless average pressure, $\bar{p}^*$, the corresponding non-contact ratio, $1 - A^*$, and average interfacial gap, $\bar{g}^*/\alpha_1^p$, are dependent only on the bandwidth parameter α^p.

7.3. Modified Greenwood's simplified elliptic model

Greenwood derived a joint PDF (see Eq. (9) in Greenwood (2006)) based on Nayak's random theory (Nayak, 1971), which is in terms of ξ_1^{h*}, s^h and r^h. ξ_1^{h*} is the dimensionless asperity height normalized by $\sqrt{m_0^h}$. s^h and r^h are the *semi-sum* and *semi-difference* of the dimensionless principle curvatures of the local asperities

$$s^h = -(\kappa_1^{h*} + \kappa_2^{h*}),\ r^h = |\kappa_1^{h*} - \kappa_2^{h*}|, \tag{57}$$

where κ_1^{h*} and κ_2^{h*} are the dimensionless (positive) semi-principle curvatures, i.e., $\kappa_i^{h*} = \kappa_i^h/\sqrt{m_4^h}, i = 1, 2$.

Assuming the rough surface is random, isotropic, and Gaussian, the joint PDF of the asperities of the "pressure surface" can be written as (see Eq. (9) in Greenwood (2006))

$$\Phi^{p*}(\xi_1^{p*}, s^p, r^p) = \frac{27}{2\pi}\sqrt{C_1}\exp\left[-C_1\left(\xi_1^{p*} + \frac{3s^p}{2\sqrt{\alpha^p}}\right)^2\right]\left[(s^p)^2 - (r^p)^2\right]r^p \exp\left[-\frac{3}{4}(s^p)^2 - \frac{3}{2}(r^p)^2\right], \tag{58}$$

where ξ_1^{p*} is the dimensionless asperity height of the "pressure surface" normalized by $\sqrt{m_0^p}$. C_1 is in terms of α^p, i.e., $C_1 = \alpha^p/(2\alpha^p - 3)$. It is obvious that the above PDF is dimensionless.

Since the expressions of non-contact region, Eq. (16), and trapped volume, Eq. (24), are in terms of κ_1^p and κ_2^p, we need to replace the variables, s^p and r^p, with κ_1^{p*} and κ_2^{p*} in the triple integrals in Eqs. (18) and (26), the following relation is needed

$$ds^p dr^p = \mathbf{J}\begin{pmatrix} s^p & r^p \\ \kappa_1^{p*} & \kappa_2^{p*} \end{pmatrix} d\kappa_1^{p*} d\kappa_2^{p*} \quad \text{if } \kappa_1^{p*} \geqslant \kappa_2^{p*}, \tag{59}$$

where $\mathbf{J}$ is the Jacobian and can be easily evaluated: $\mathbf{J}(\bullet) = 2$. κ_1^{p*} and κ_2^{p*} now denote the dimensionless asperities curvatures of the "pressure surface" i.e., $\kappa_i^{p*} = \kappa_i^p/\sqrt{m_4^p}, i = 1, 2$.

Consequently, the PDF in terms of $\xi_1^{p*}, \kappa_1^{p*}$ and κ_2^{p*} is

$$\Phi^{p*}(\xi_1^{p*}, \kappa_1^{p*}, \kappa_2^{p*}) = \frac{108}{\pi}\sqrt{C_1}\exp\left\{-C_1\left[\xi_1^{p*} - \frac{3(\kappa_1^{p*} + \kappa_2^{p*})}{2\sqrt{\alpha^p}}\right]^2\right\}\kappa_1^{p*}\kappa_2^{p*}(\kappa_1^{p*} - \kappa_2^{p*}) \times \exp\left\{-\frac{9}{4}\left[(\kappa_1^{p*})^2 + (\kappa_2^{p*})^2 - \frac{2}{3}\kappa_1^{p*}\kappa_2^{p*}\right]\right\}. \tag{60}$$

Rewriting Eqs. (16) and (24) in terms of dimensionless variables $\xi_1^{p*}, \kappa_1^{p*}$ and κ_2^{p*}, we have

$$\overline{A}_i = \frac{3}{2}\pi\frac{\sqrt{m_0^p}}{\sqrt{m_4^p}}\frac{\xi_1^{p*} - \bar{p}^*}{\sqrt{\kappa_1^{p*}\kappa_2^{p*}}}, \tag{61}$$

and

$$\overline{V}_i = \frac{16\sqrt{3}}{5\sqrt{2}\pi E^*}\frac{(m_0^p)^{5/4}}{(m_4^p)^{3/4}}\frac{(\xi_1^{p*} - \bar{p}^*)^{5/2}}{\kappa_1^{p*}\sqrt{\kappa_2^{p*}}}\mathbf{E}(e), \tag{62}$$

where the eccentricity is $e = \sqrt{1 - \kappa_2^{p*}/\kappa_1^{p*}}$.

Consequently, substituting Eqs. (60)–(62) into Eqs. (18) and (26), the contact ratio, A^*, is then

$$1 - A^*(\bar{p}^*) = \frac{(\alpha^p)^{1/2}}{4\sqrt{3}}\int_{\bar{p}^*}^{\infty}\int_{0}^{\infty}\int_{0}^{\kappa_1^{p*}}\frac{(\xi_1^{p*} - \bar{p}^*)}{\sqrt{\kappa_1^{p*}\kappa_2^{p*}}}\Phi^{p*}(\xi_1^{p*}, \kappa_1^{p*}, \kappa_2^{p*})d\kappa_2^{p*}d\kappa_1^{p*}d\xi_1^{p*}, \tag{63}$$

and the average interfacial gap, $\bar{g}^*$, is

$$\bar{g}^*(\bar{p}^*)/\alpha_1^p = \frac{8}{15\sqrt{2}\pi^2}(\alpha^p)^{1/4}\int_{\bar{p}^*}^{\infty}\int_{0}^{\infty}\int_{0}^{\kappa_1^{p*}} \times \frac{(\xi_1^{p*} - \bar{p}^*)^{5/2}}{\kappa_1^{p*}\sqrt{\kappa_2^{p*}}}\mathbf{E}(e)\Phi^{p*}(\xi_1^{p*}, \kappa_1^{p*}, \kappa_2^{p*})d\kappa_2^{p*}d\kappa_1^{p*}d\xi_1^{p*}. \tag{64}$$

where $\alpha_1^p = \frac{m_0^p}{\sqrt{m_2^p}}\frac{1}{E^*\sigma}$.

Note that a similar observation to that declared in the ends of Sections 7.1,2: for a fixed dimensionless average pressure, $\bar{p}^*$, the corresponding non-contact ratio, $1 - A^*$, and average interfacial gap, $\bar{g}^*/\alpha_1^p$, are dependent only on the bandwidth parameter α^p. Additionally, the modified Greenwood model is, so far, the most complete statistical model among all the newly developed models.

8. Numerical results

In the previous sections, three statistical models are developed (see Section 7) for the case of nearly complete contact based on the GW, Nayak–Bush and Greenwood's simplified elliptic contact models. All three newly developed models are referred to as *modified statistical models*. In this section, the numerical results of the following models are discussed:

1. "Original GW model": Statistical model developed by Greenwood and Williamson (1966);
2. "Modified GW model": Statistical model (Eqs. (44) and (45)) based on original GW model applied in the case of nearly complete contact, see Section 7.1;
3. "Original Nayak–Bush model": Statistical model developed by Bush based on Nayak's random theory (Bush and Thomas, 1982);
4. "Modified Nayak–Bush model": Statistical model (Eqs. (55) and (56)) based on the Nayak–Bush model applied in the case of nearly complete contact, see Section 7.2;
5. "Original Greenwood model": Greenwood's simplified elliptic model based on Nayak's random theory and Hertzian mildly elliptic contact model (Greenwood, 2006);
6. "Modified Greenwood model": Statistical model (Eqs. (63) and (64)) based on Greenwood's simplified elliptic model applied in the case of nearly complete contact, see Section 7.3;
7. "Persson's theory of contact": Persson's model for nominally flat elastic rough surfaces contact (Persson, 2002; Manners and Greenwood, 2006).

Since to flatten a rough surface an infinite average pressure is needed, we should find a reasonable range of $\bar{p}^*$ in which nearly complete contact occurs. According to the Gaussian PDF of the complete contact pressure distribution, see Eq. (35), the following range

$$\bar{p}^* = [0, m^p + 3\sigma_s^p]/\sqrt{m_0^p}. \tag{65}$$

may be used as an effective range of the variation of the dimensionless average pressure, $\bar{p}^*$. The value of the non-contact ratio, $1 - A^*$, at nearly complete contact is restricted to the range of $[0, 0.1]$. This rough quantified range is only made to simplify the discussion below. Before we discuss the solutions of the modified statistical models, Persson's theory of contact also needs to be introduced briefly.

According to Manners and Greenwood (2006), Persson's theory of contact gives the following simple form of contact ratio to average pressure relation for the nominally flat rough contact:

$$A^* = \mathrm{erf}\left(\bar{p}/\sqrt{2V}\right), \tag{66}$$

where erf() is the *error function*. $V = m_0^p$ is the variance of the pressure distribution, $p = p_c(x, y)$, at the case of complete contact.[3] Consequently, the above equation can be rewritten as

$$1 - A^*(\bar{p}^*) = \mathrm{erfc}(\bar{p}^*/\sqrt{2}), \tag{67}$$

where erfc() is the *complementary error function*. $\bar{p}^*$ is the dimensionless average pressure normalized by $\sqrt{m_0^p}$.

Fig. 8 shows the non-contact ratio, $1 - A^*$, to dimensionless average pressure, $\bar{p}^*$, relations predicted by the modified statistical models and Persson's theory of contact. For both cases considered, $\alpha^p = 2$ and $\alpha^p = 10$, the nearly complete contact models all start approximately from $\bar{p}^* = 1$. Let us focus on the range $\bar{p}^* \geqslant 1$ in Fig. 8(a) and (b). All three statistical models have nearly the same predictions and gradually converge into an apparent universal relation at extremely high loads, although those models differ from Persson's theory of contact in the early contact region (at low loads). Note that Persson's theory of contact is claimed to be exact for complete contact but may not be for lower loads. Since Persson's model agrees qualitatively with the modified statistical models in the majority of the range of the nearly complete contact, especially at extremely high load, they help confirm the validity of each other to some extent. We can expect that the gaps will gradually decrease and eventually close when $\bar{p}^*$ reaches infinity. In the proceeding sections, we have the same observations for all the modified statistical models that for a fixed $\bar{p}^*$, the non-contact ratio, $1 - A^*$, is only in terms of α^p. In Persson's theory of contact, however, the non-contact ratio, $1 - A^*$, is constant for a fixed $\bar{p}^*$, see Eq. (67). For the case of low α^p ($\alpha^p = 2$), modified statistical models follow closer to Persson's theory of contact than that for the case of high α^p ($\alpha^p = 10$).

Fig. 9 illustrates the detailed comparisons between the modified statistical models. Predictions of the non-contact ratio, $1 - A^*$, to dimensionless average pressure relation, $\bar{p}^*$, showed in Fig. 9(a) and (c) are very close to each other, especially at the heavy load range and for the cases with higher bandwidth parameter, α^p. In Fig. 9(b) and (d), the slopes of the relations between the non-contact ratio, $1 - A^*$, and the dimensionless average interfacial gap, $\bar{g}^*/\alpha_1^p$, predicted by modified statistical models are all slightly off the unity at nearly complete contact regime, which indicates mildly nonlinear relations for both cases, $\alpha^p = 2$ and $\alpha^p = 10$. As α^p increases, this non-linearity becomes more severe (slope is 1.11 for $\alpha^p = 2$ and 1.14 for $\alpha^p = 10$). In Fig. 9(b) and (d), the prediction of the modified GW model is below that of modified Nayak–Bush and modified Greenwood models, both of which are having nearly the same predictions for both cases: $\alpha^p = 2$ and $\alpha^p = 10$.

9. Discussions

9.1. Analogies between the statistical models at early and nearly complete contact

Let us focus on the original Nayak–Bush and modified Nayak–Bush models. Rewriting the contact ratio, A^*, to surface separation, d^*, relation

$$A^*(d^*) = \frac{\sqrt{\alpha^h}}{6\sqrt{3}} \int_{d^*}^{\infty} \int_{-\infty}^{0} (\xi_1^{h*} - d^*)(-u^h)^{-1} \Phi^{h*}(\xi_1^{h*}, u^h) du^h d\xi_1^{h*}, \tag{C.9}$$

in the original Nayak–Bush model and non-contact ratio, $1 - A^*$, to average pressure, $\bar{p}^*$, relation

$$1 - A^*(\bar{p}^*) = \frac{\sqrt{\alpha^p}}{2\sqrt{3}} \int_{\bar{p}^*}^{\infty} \int_{-\infty}^{0} (\xi_1^{p*} - \bar{p}^*)(-u^p)^{-1} \Phi^{p*}(\xi_1^{p*}, u^p) du^p d\xi_1^{p*}, \tag{55}$$

in the modified Nayak–Bush model. If we check the expressions of Φ^{p*} (Eq. (49)) and Φ^{h*} (Eq. (C.7)), we may find that except for the different constant terms outside the integrals, the right hand side of the above two equations are exactly the same by replacing the variables, ξ_1^{p*}, u^p and $\bar{p}^*$, with ξ_1^{h*}, u^h and d^* in Eq. (55). Similar analogies can also be found in the other statistical model pairs, e.g., original Greenwood and modified Greenwood models.

Fig. 10 shows the detailed comparisons between the classic statistical models for low loads. Similar patterns in Fig. 9 can be found here. The classic statistical models have nearly the same predictions of the contact ratio, A^*, to surface separation, d^*, relations, especially at the early contact where the contact ratio is infinitesimally small, see Fig. 10(a) and (c). The contact ratio, A^*, to dimensionless contact load, $P^*/\sqrt{m_2^h}$, relation is linear (at least very close to linearity) at early contact when A^* is vanishing. This phenomenon is widely accepted and explored in details by Carbone and Bottiglione (2008).

Rewriting the contact load, P^*, to surface separation, d^*, relation

$$P^*(d^*) \Big/ \sqrt{m_2^h} = \frac{2}{9\sqrt{3}\pi} (\alpha^h)^{3/4} \int_{d^*}^{\infty} \int_{-\infty}^{0} (\xi_1^{h*} - d^*)^{3/2} (-u^h)^{-1/2} \Phi^{h*}(\xi_1^{h*}, u^h) du^h d\xi_1^{h*}, \tag{D.8}$$

in the original Nayak–Bush model and the average interfacial gap, $\bar{g}^*/\alpha_1^p$, to the average pressure, $\bar{p}^*$, relation

[3] Here we implicitly assume that the statistics of the "pressure distribution", $p = \pm p_c(x, y)$, are the same.

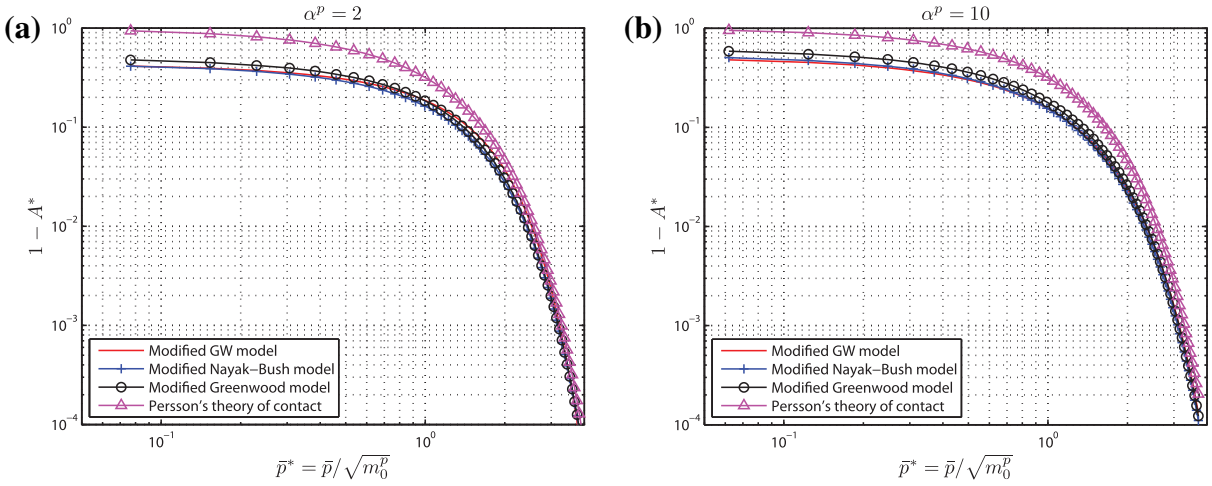

Fig. 8. Non-contact ratio, $1 - A^*$, to dimensionless average pressure, $\bar{p}^*$, relations for two cases: (a) $\alpha^p = 2$ and (b) $\alpha^p = 10$.

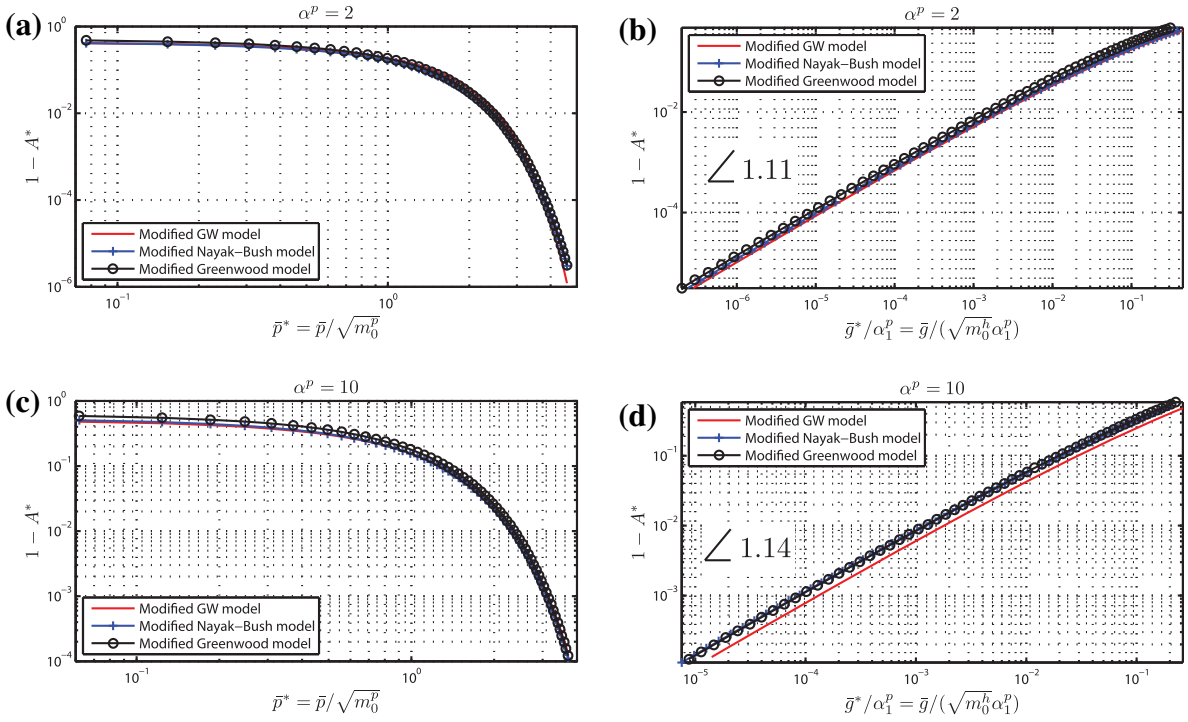

Fig. 9. Non-contact ratio, $1 - A^*$, to dimensionless average pressure, $\bar{p}^*$, relations for (a) $\alpha^p = 2$ and (c) $\alpha^p = 10$; Non-contact ratio, $1 - A^*$, to dimensionless average interfacial gap, $\bar{g}^*$, for (b) $\alpha^p = 2$ and (d) $\alpha^p = 10$.

$$\bar{g}^*(\bar{p}^*)/\alpha_1^p = \frac{8}{15\pi}(\alpha^p)^{1/4}\int_{\bar{p}^*}^{\infty}\int_{-\infty}^{0}(\xi_1^{p*} - \bar{p}^*)^{5/2}(-u^p)^{-3/2}\Phi^{p*}(\xi_1^{p*}, u^p)du^p d\xi_1^{p*}, \tag{56}$$

in the modified Nayak–Bush model. Higher powers (5/2 and 3/2) of both terms: ξ_1^{p*} and $(-u^p)^{-1}$ when compared to (3/2 and 1/2) of ξ_1^{h*} and $(-u^h)^{-1}$ cause more severe non-linearity as shown in Fig. 9(b) and (d).

9.2. Connections between the statistical models at early and nearly complete contact

When we are trying to connect these two different kinds of statistical models: the classic and modified statistical models, which describe the two extreme cases, namely, the early and nearly complete contact, we meet a contrasting situation where d^* (variable in classic statistical models) and $\bar{g}^*$ (variable in modified statistical model) has different meaning. In the following paragraph, we will show that $\bar{g}^*$ and d^* are indeed approximately equivalent at nearly complete contact.

In the classic statistical models, e.g., the GW model, d^* is defined as the dimensionless surface separation between the mean level of the *undeformed* rough surface and the rigid flat, which equivalent to assuming that the substrate is *rigid* and only asperities superposed on it are *elastic*. This assumption is introduced because an accurate description of the elasticity of the substrate is difficult under the framework of the statistical models, except in an average sense (Zhao and Chang, 2001; Ciavarella et al., 2008).

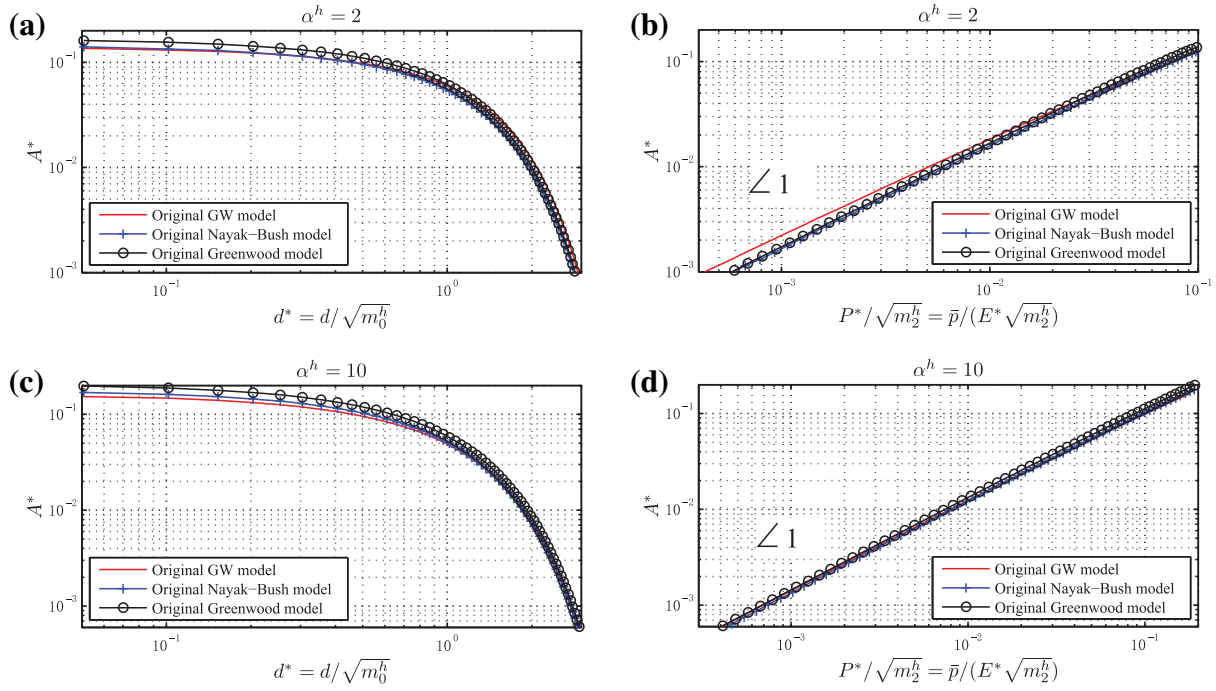

Fig. 10. Contact ratio, A^*, to dimensionless surface separation, d^*, relations for (a) $\alpha^h = 2$ and (c) $\alpha^h = 10$; Contact ratio, A^*, to dimensionless contact load, P^*, for (b) $\alpha^h = 2$ and (d) $\alpha^h = 10$.

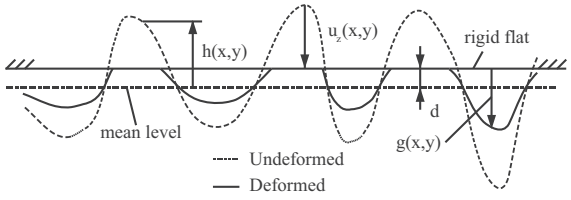

Fig. 11. Schematic representation of the surface separation between the rigid flat and deformed rough surface. Note that the uniform (rigid body) displacement of the rough surface (the rigid flat) is neglected.

Let us redefine d^* as the surface separation between the rigid flat and the mean level of the *deformed* rough surface, see Fig. 11. Note that the uniform (rigid body) displacements of the rough surface and rigid flat are neglected in Fig. 11. This new definition of d^* abandons the rigidity of the substrate and is still valid for the classic statistical models applied at early contact since local asperity deformations are dominant comparing to that of the substrate. As d^* is decreased from infinity to zero, the rough contact transits from first touch to complete contact.

Average interfacial gap is defined as: $\bar{g}^* = \frac{1}{\sigma}\int_\Omega g(x,y)dA$ where $g(x,y)$ is the gap between the *deformed* surface and the rigid flat at (x,y), see Fig. 11. Since we neglect the uniform (rigid body) displacement of the rough surface and rigid flat, i.e., $E[u_z] = 0$, the following relation between $\bar{g}^*$ and d^* is exact:

$$\bar{g}^* = d^* - \frac{1}{\sigma}\int_\Omega h(x,y) - u_z(x,y)dA. \tag{68}$$

As d^* is decreased, especially at nearly complete contact, the difference between $u_z(x,y)$ and $h(x,y)$ are more and more smaller. Thus, $\int_\Omega h(x,y) - u_z(x,y)dA \to 0$ when non-contact area, $1 - A^*$, is vanishing and finally we have

$$\bar{g}^* = d^*. \tag{69}$$

The above identity ensures that the classic statistical models and the modified statistical model are two *asymptotic* solutions of a universal statistical contact model.

9.3. Limitations of numerical deterministic model

Numerical deterministic models (Stanley and Kato, 1997, e.g., Polonsky and Keer, 2000; Liu et al., 1999) are not applied here to validate the newly developed statistical models, since it is likely to have inaccurate predictions when non-contact area, $1 - A^*$, is vanishing because of the insufficient population of (1) non-contact regions and (2) sampling points within each of them. Hyun et al. (2004) pointed out that the finite element (FE) model of the elastic rough surface contact is also not accurate when A^* is vanishing due to the insufficient number of contact regions and sampling points within each of them.

The newly developed statistical models solve the problem of insufficient non-contact regions by using a continuous PDF to describe the distribution of the asperities of the "pressure surface". The problem of insufficient sampling points in each non-contact region is solved by introducing the concept of a "crack" which has a certain deterministic profile. Consequently, the newly developed statistical models must have a broader range of application and better accuracy than the numerical deterministic models in nearly complete contact (when $1 - A^*$ is vanishing).

10. Conclusion

In the current work, the problem of the elastic contact between a homogeneous, isotropic, linear elastic half-space with a nominally flat geometrically-isotropic rough surface on the boundary and a rigid flat is solved at nearly complete contact. By introducing the concept of a penny-shaped crack and the stress intensity factor, the area of each non-contact region and the trapped volume formed within each "crack" are determined respectively based on the geometrical parameters (e.g., height and principle curvatures) of the asperities of the "pressure surface". Knowing the PDF of the asperities of the "pressure surface", statistical models, built under the framework of the GW, Nayak–Bush and Greenwood's simplified elliptic models, are applied to determine the relations between the contact ratio, A^*, average pressure, $\bar{p}^*$, and average

interfacial gap, $\bar{g}^*$, at nearly complete contact. The non-contact ratio, $1-A^*$, to the average pressure, $\bar{p}^*$, relations from the newly developed statistical models have a good qualitative agreement with that of Persson's theory of contact at the majority of the range of the nearly complete contact. Three different statistical models, namely, the modified GW, modified Nayak–Bush and modified Greenwood's simplified models, have similar predictions of (i) the non-contact ratio, $1-A^*$, to the average pressure, $\bar{p}^*$, relation and (ii) the non-contact ratio, $1-A^*$, to the average interfacial gap, $\bar{g}^*$. Similar patterns of the corresponding relation curves have been found in the statistical models applied at both early and nearly complete contact cases. Finally, we find that the classic statistical models and the newly developed models represent two asymptotic solutions of a universal rough surface contact model valid throughout the whole load range from first touch to complete contact.

Appendix A. Analytical pressure distribution at complete contact

Johnson et al. (1985) derived the analytical solution of a spatial contact problem of an elastic half-space with slightly bi-sinusoidal waviness in contact with a rigid flat at complete contact based on the *Westergaard solution* (Westergaard, 1939)

$$p(x,y)=\hat{p}\cos(w_x x)\cos(w_y y),$$

$$\Updownarrow \text{ gives rise to}$$

$$u_z(x,y)=\Delta\cos(w_x x)\cos(w_y y), \tag{A.1}$$

where $\hat{p}=\frac{1}{2}E^*\Delta\sqrt{w_x^2+w_y^2}$ is the average pressure at complete contact. w_x and w_y are the frequencies in the x and y directions.

Assume the surface displacement field is $u_z(x,y)=h(x,y)$ with $E[h]=0$. According to the above correlation, the pressure distribution p_c corresponding to the surface displacement field, $u_z(x,y)=h(x,y)$, can be derived through the Fourier transform (Stanley and Kato, 1997)

$$p_c(x,y)=\mathcal{F}^{-1}\left[\frac{1}{2}E^*\sqrt{w_x^2+w_y^2}\mathcal{F}[h(x,y)]\right], \tag{A.2}$$

where $\mathcal{F}[\bullet]$ and $\mathcal{F}^{-1}[\bullet]$ are the operators of Fourier transform and its inverse. It is obvious to see that $E[p_c]=0$ as long as $E[h]=0$.

Appendix B. Derivation of interfacial crack area

A penny-shaped crack, Fig. 7(c), under the action of an axisymmetric pressure distribution, $p_2(\rho)=(p-\bar{p})-\kappa_1 b_n^2\rho^2$, has been studied by Sneddon (1946) and the resultant crack opening displacement, $g(\rho)$, can be obtained through a closed-form recurrence relation (Sneddon, 1946; Johnson et al., 1985). The details of the derivation of $g(\rho)$ can be found in Johnson et al. (1985, Appendix 2). Here only the final expression of $g(\rho)$ is given:

$$g(\rho)=\frac{4b_n}{9\pi E^*}[9(p-\bar{p})-2b_n^2\kappa_1-4b_n^2\kappa_1\rho^2](1-\rho^2)^{1/2}. \tag{B.1}$$

Since there's no singularity at the edges of the contact region, the crack surface separates smoothly, i.e., the derivative $dg(r)/dr=0$ when $r=b_n$. The terms in the square bracket must be zero in order to satisfied the above smoothness condition. Thus, we have the

$$b_n=\sqrt{\frac{3(p-\bar{p})}{2\kappa_1}}, \tag{B.2}$$

which is the same as that in Eq. (14) derived by Manners and Greenwood (2006).

Appendix C. Classic statistical models

C.1. McCool's input

The original McCool's input (McCool, 1987) is applied to quantify the input of the original GW model which can be stated in the following form:

$$\eta^h=\frac{1}{6\sqrt{3}\pi}\left(\frac{m_4^h}{m_2^h}\right),\quad m^h=4\left(\frac{m_0^h}{\pi\alpha^h}\right)^{1/2},$$
$$R^h=0.375\left(\frac{\pi}{m_4^h}\right)^{1/2},\quad \sigma_s^h=\left(1-\frac{0.8968}{\alpha^h}\right)^{1/2}(m_0^h)^{1/2}, \tag{C.1}$$

where η_s^h is the asperity density. R^h is the average radius of curvatures of the asperities. σ_s^h is the root mean square (r.m.s) roughness of the asperities. m^h is the distance between the mean asperity level and the mean level. $m_i^h, i=0,2,4$, are the spectral moments of the rough surface. α^h is the bandwidth parameter: $\alpha^h=\frac{m_0^h m_4^h}{(m_2^h)^2}$.

C.2. Original Greenwood–Williamson (GW) Model

The original Greenwood–Williamson (GW) model (Greenwood and Williamson, 1966) consists of two integral equations for dimensionless contact load, $P^*=P/(E^*A_n)$, and contact ratio, $A^*=A/A_n$,

$$P^*(d^*)=\eta_s^h\frac{4}{3}\sqrt{R^h}(\sigma_s^h)^{5/2}\int_{d^*}^{\infty}(\xi_1^{h*}-d^*)^{3/2}\Phi^h(\xi_1^{h*})d\xi_1^{h*},$$
$$A^*(d^*)=\eta_s^h\pi R^h(\sigma_s^h)^2\int_{d^*}^{\infty}(\xi_1^{h*}-d^*)\Phi^h(\xi_1^{h*})d\xi_1^{h*}, \tag{C.2}$$

where $d^*=d/\sigma_s^h$ is the dimensionless surface separation between the rigid flat and the mean level of the rough surface. $\xi_1^{h*}=\xi_1^h/\sigma_s^h$ is the dimensionless asperity height. $\Phi^h(\xi_1^{h*})$ is a Gaussian probability density function (PDF) of the asperities distribution

$$\Phi^h(\xi_1^{h*})=\frac{1}{\sqrt{2\pi}\sigma_s^h}\exp\left[-\frac{\left(\xi_1^{h*}\sigma_s^h-m^h\right)^2}{2(\sigma_s^h)^2}\right], \tag{C.3}$$

Defining the dimensionless Gaussian distribution

$$\Phi^{h*}(\xi_1^{h*})=\sigma_s^h\Phi^h(\xi_1^{h*})=\frac{1}{\sqrt{2\pi}}\exp\left[-\frac{\left(\xi_1^{h*}\sigma_s^h-m^h\right)^2}{2(\sigma_s^h)^2}\right], \tag{C.4}$$

and substituting McCool's input (Eq. (C.1)) and Eq. (C.4) into Eqs. (C.2) we have

$$P^*(d^*)/\sqrt{m_2^h}=\frac{1}{9\sqrt{2}(\pi)^{3/4}}(\alpha^h-0.8968)^{3/4}\int_{d^*}^{\infty}(\xi_1^{h*}-d^*)^{3/2}\Phi^{h*}(\xi_1^{h*})d\xi_1^{h*},$$
$$A^*(d^*)=\frac{\sqrt{3\pi}}{48}\sqrt{\alpha^h-0.8968}\int_{d^*}^{\infty}(\xi_1^{h*}-d^*)\Phi^{h*}(\xi_1^{h*})d\xi_1^{h*}. \tag{C.5}$$

For a given dimensionless surface separation, d^*, according to Eq. (C.5), the corresponding contact ratio, A^*, and the dimensionless contact load, $P^*/\sqrt{m_2^h}$, only in terms of α^h. In the following statistical model, d^* is normalized by $\sqrt{m_0^h}$, while here d^* is normalized by σ_s^h. Since $\sigma_s^h=\left(1-\frac{0.8968}{\alpha^h}\right)^{1/2}(m_0^h)^{1/2}$, the truth, that the dimensionless contact load, $P^*(d^*)/\sqrt{m_2^h}$, and contact ratio, $A^*(d^*)$, are only dependent on α^h, will still hold if d^* used in the GW model is normalized by $\sqrt{m_0^h}$ in stead of σ_s^h.

C.3. Original Nayak–Bush Model

Bush and Thomas (1982) applied the joint PDF (Eq. (61) in Nayak (1971)) derived by Nayak, in the following statistical model:

$$P^*(d^*)=\eta^h\frac{4}{3}\left[\frac{(m_0^h)^3}{m_4^h}\right]^{1/4}\int_{d^*}^{\infty}\int_{-\infty}^{0}(\xi_1^{h*}-d^*)^{3/2}(-u^h)^{-1/2}\Phi^{h*}(\xi_1^{h*},u^h)du^h d\xi_1^{h*},$$
$$A^*(d^*)=\eta^h\pi\sqrt{m_0^h}m_4^h\int_{d^*}^{\infty}\int_{-\infty}^{0}(\xi_1^{h*}-d^*)(-u^h)^{-1}\Phi^{h*}(\xi_1^{h*},u^h)du_h d\xi_1^{h*}, \quad (C.6)$$

where the dimensionless joint PDF, $\Phi^{h*}(\xi_1^{h*},u^h)$, is

$$\Phi^{h*}(\xi_1^{h*},u^h)=\frac{3\sqrt{C_1}}{2\pi}\exp\left[-C_1(\xi_1^{h*})^2\right]\times\left\{3(u^h)^2-2+2\exp\left[-\frac{3}{2}(u^h)^2\right]\right\}\exp\left\{-\frac{1}{2}\left[3C_1(u^h)^2+\sqrt{3}C_2u^h\xi_1^{h*}\right]\right\}, \quad (C.7)$$

where ξ_1^{h*} and d^* are the dimensionless asperity height and surface separation normalized by $\sqrt{m_0^h}$, respectively. u^h is a dimensionless average curvature, $u^h=-\kappa_m/\sqrt{m_4^h}$.

Substituting McCool's input (Eq. (C.1)) into Eqs. (C.6), we have

$$P^*(d^*)/\sqrt{m_2^h}=\frac{2}{9\sqrt{3}\pi}(\alpha^h)^{3/4}\int_{d^*}^{\infty}\int_{-\infty}^{0}(\xi_1^{h*}-d^*)^{3/2}(-u^h)^{-1/2}\Phi^{h*}(\xi_1^{h*},u^h)du^h d\xi_1^{h*}, \quad (C.8)$$

$$A^*(d^*)=\frac{\sqrt{\alpha^h}}{6\sqrt{3}}\int_{d^*}^{\infty}\int_{-\infty}^{0}(\xi_1^{h*}-d^*)(-u^h)^{-1}\Phi^{h*}(\xi_1^{h*},u^h)du^h d\xi_1^{h*}. \quad (C.9)$$

For a given dimensionless surface separation, d^*, according to Eqs. (C.8) and (C.9), the corresponding contact ratio, A^*, and the dimensionless contact load, $P^*/\sqrt{m_2^h}$, only in terms of α^h, see Eqs. (C.8) and (C.9).

C.4. Original Greenwood's Simplified Elliptic Model

Greenwood (2006) obtained the following integral equations for both dimensionless contact load, P^*, and contact ratio, A^*, as an approximation to the BGT model (Bush et al., 1975)

$$P^*(d^*)=\eta^h\pi\sqrt{\frac{m_0^h}{m_4^h}}\int_{d^*}^{\infty}\int_{0}^{\infty}(\xi_1^{h*}-d^*)^{3/2}\left(\kappa_g^*\right)^{-1/2}\Phi^{h*}(\xi_1^{h*},\kappa_g^*)d\kappa_g^* d\xi_1^{h*},$$
$$A^*(d^*)=\eta^h\frac{4}{3}\left[\frac{(m_0^h)^3}{m_2^h}\right]^{1/4}\int_{d^*}^{\infty}\int_{0}^{\infty}(\xi_1^{h*}-d^*)\left(\kappa_g^*\right)^{-1}\Phi^{h*}(\xi_1^{h*},\kappa_g^*)d\kappa_g^* d\xi_1^{h*}, \quad (C.10)$$

where the dimensionless joint PDF, $\Phi^{h*}(\xi^*,\kappa_g^*)$ is

$$\Phi^{h*}(\xi_1^{h*},\kappa_g^*)=\frac{9}{2\sqrt{2\pi}}\sqrt{\frac{\alpha^h}{\alpha^h-1}}\left(\kappa_g^*\right)^3\mathrm{erfc}\left\{\sqrt{\frac{\alpha^h-1}{2(2\alpha^h-3)}}\left[3\kappa_g^*-\frac{\xi_1^{h*}\sqrt{\alpha^h}}{\alpha^h-1}\right]\right\}\times\exp\left[\frac{-\alpha^h(\xi_1^{h*})^2}{2(\alpha^h-1)}+\frac{3(\kappa_g^*)^2}{2}\right], \quad (C.11)$$

κ_g^* is a dimensionless geometric curvature κ_g, i.e., $\kappa_g^*=\kappa_g^h/\sqrt{m_4^h}$. ξ_1^{h*} is a dimensionless asperity height, i.e., $\xi_1^{h*}=\xi_1^h/\sqrt{m_0^h}$. d^* is dimensionless surface separation, $d^*=d/\sqrt{m_0^h}$. erfc() is the *complementary error function*.

Substituting McCool's input (Eq. (C.1)) into Eqs. (C.10), we have

$$P^*(d^*)/\sqrt{m_2^h}=\frac{2(\alpha^h)^{3/4}}{9\sqrt{3}\pi}\int_{d^*}^{\infty}\int_{0}^{\infty}(\xi_1^{h*}-d^*)^{3/2}\left(\kappa_g^*\right)^{-1/2}\Phi^{h*}(\xi_1^{h*},\kappa_g^*)d\kappa_g^* d\xi_1^{h*},$$
$$A^*(d^*)=\frac{\sqrt{\alpha^h}}{6\sqrt{3}}\int_{d^*}^{\infty}\int_{0}^{\infty}(\xi_1^{h*}-d^*)\left(\kappa_g^*\right)^{-1}\Phi^{h*}(\xi_1^{h*},\kappa_g^*)d\kappa_g^* d\xi_1^{h*}. \quad (C.12)$$

Again we notice that, for a given dimensionless surface separation, d^*, the corresponding contact ratio, A^*, and the dimensionless contact load, $P^*/\sqrt{m_2^h}$, are only in terms of α^h, see Eqs. (C.12).

References

Archard, J.F., 1957. Elastic Deformation and the Laws of Friction. Proc. Roy. Soc. A 243, 190–205.

Barber, J.R., 2003. Bounds on the electrical resistance between contacting elastic rough bodies. Proc. R. Soc. Lond. A 459, 53–66.

Barenblatt, G.I., 1962. The mathematical theory of equilibrium cracks in brittle fracture. Adv. Appl. Mech. 7, 55–129.

Buckner, H.F., 1958. The propagation of cracks and the energy of elastic deformation. ASME J. Appl. Mech. 80, 1225–1230.

Bush, A.W., 1982. Contact mechanics. In: Thomas, T.R. (Ed.), Rough Surfaces, First ed. Longman, London.

Bush, A.W., Gibson, R.D., Thomas, T.R., 1975. The elastic contact of a rough surface. Wear 19, 163–168.

Bush, A.W., Gibson, R.D., Keogh, G.P., 1976. The limit of elastic deformation in the contact of rough surfaces. Mech. Res. Commun. 3, 169–174.

Carbone, G., Bottiglione, F., 2008. Asperity contact theories: Do they predict linearity between contact area and load? J. Mech. Phys. Solids 56, 2555–2572.

Ciavarella, M., Demelio, G., Barber, J.R., Jang, Y.H., 2000. Linear elastic contact of the weierstrass profile. Proc. R. Soc. Lond. A 456, 387–405.

Ciavarella, M., Greenwood, J.A., Paggi, M., 2008. Inclusion of interaction in the Greenwood and Williamson contact theory. Wear 265, 729–734.

Francis, H.A., 1977. Application of spherical indentation mechanics to reversible and irreversible contact between rough surfaces. Wear 45, 221–269.

Greenwood, J.A., 2006. A simplified elliptic model of rough surface contact. Wear 261, 191–200.

Greenwood, J.A., Williamson, J.B.P., 1966. Contact of Nominally Flat Surfaces. Proc. R. Soc. London Ser. A 295, 300–319.

Hyun, S., Pei, L., Molinari, J.F., Robbins, M., 2004. Finite element analysis of contact between elastic self-affine surfaces. Phy. Rev. E 70, 026117.

Jackson, R.L., 2011. An analytical solution to an archard-type fractal rough surface contact model. Tribol. Trans. 53, 543–553.

Johnson, K.L., Greenwood, J.A., Higginson, J.G., 1985. The contact of elastic regular wavy surfaces. Int. J. Mech. Sci. 27 (6), 383–396.

Kudish, I.I., Cohen, D.K., Vyletel, B., 2013. Perfect mechanical sealing in rough elastic contacts: Is it possible? ASME J. Appl. Mech. 80, 014504.

Liu, G., Wang, Q., Lin, C., 1999. A survey of current models for simulating the contact between rough surfaces. Tribol. Trans. 42 (3), 581–591.

Manners, W., 2000. Pressure required to flatten an elastic random rough profile. Int. J. Mech. Sci. 42, 2321–2336.

Manners, W., Greenwood, J.A., 2006. Some observations on Persson's diffusion theory of elastic contact. Wear 261, 600–610.

McCool, J.I., 1987. Relating profile instrument measurements to the functional performace of rough surfaces. ASME J. Tribol. 109, 264–270.

McCool, J.I., Gassel, S.S., 1981. The contact of two surfaces having anisotropic roughness geometry. ASLE. Spec. Publ. SP-7, 29–38.

Nayak, P.R., 1971. Random Process Model of Rough Surfaces. ASME J. Lub. Tech. 93, 398–407.

O'Callaghan, M., Cameron, M.A., 1976. Static contact under load between nominally flat surfaces in which the deformation is purely elastic. Wear 36, 79–97.

Persson, B.N.J., 2002. Theory of rubber friction and contact mechanics. J. Chem. Phys. 115, 3840–3861.

Persson, B.N.J., 2007. Relation between interfacial separation and load: a general theory of contact mechanics. Phys. Rev. Lett. 99, 125502.

Polonsky, I.A., Keer, L.M., 2000. Fast methods for solving rough contact problems: a comparative study. ASME J. Tribol. 122 (1), 36–41.

Salganik, R.L., Mokhel, A.N., Fedotov, A.A., 2009. Contact problems for rough elastic solids being in nearly full contact or regarded as such for further elaboration. J. Phys.: Conf. Ser. 181, 012012.

Sneddon, I.N., 1946. The distribution of stress in the neighborhood of a crack in an elastic solid. Proc. R. Soc. Lond. A 187, 229–260.

Stanley, H.M., Kato, T., 1997. An FFT-based method for rough surface contact. ASME J. Tribol. 119, 481–485.

Westergaard, H.M., 1939. Bearing pressure and cracks. ASME J. Appl. Mech. 6, 49–53.

Zhao, Y., Chang, L., 2001. A model of asperity interactions in elastic–plastic contact of rough surfaces. ASEM J. Tribol. 123, 857–864.